

## Geological Desktop Summary

Active Permit areas 50753 (55581), 54068 and 54272, South  
Taranaki Bight

Prepared for Trans-Tasman Resources Limited

Updated November 2015

**Authors/Contributors:**

Alan R. Orpin

**For any information regarding this report please contact:**

Alan Orpin  
Marine Sedimentologist  
Ocean Sediments  
+64-4-386 0356  
alan.orpin@niwa.co.nz

National Institute of Water & Atmospheric Research Ltd  
301 Evans Bay Parade, Greta Point  
Wellington 6021  
Private Bag 14901, Kilbirnie  
Wellington 6241  
New Zealand

Phone +64-4-386 0300  
Fax +64-4-386 0574

NIWA Client Report No: WLG2013-44  
Report date: August 2013  
NIWA Project: TTR11301

---

© All rights reserved. This publication may not be reproduced or copied in any form without the permission of the copyright owner(s). Such permission is only to be given in accordance with the terms of the client's contract with NIWA. This copyright extends to all forms of copying and any storage of material in any kind of information retrieval system.

Whilst NIWA has used all reasonable endeavours to ensure that the information contained in this document is accurate, NIWA does not give any express or implied warranty as to the completeness of the information contained herein, or that it will be suitable for any purpose(s) other than those specifically contemplated during the Project or agreed by NIWA and the Client.

# Contents

<b>Executive summary</b> .....	<b>6</b>
<b>1 Overview</b> .....	<b>8</b>
1.1 Current ironsand mining .....	8
1.2 Scope of work .....	10
1.3 Project brief.....	10
<b>2 Data Discovery</b> .....	<b>11</b>
2.1 Data sources.....	11
<b>3 Environmental setting</b> .....	<b>15</b>
3.1 Ocean circulation .....	15
3.2 Waves.....	16
3.3 Sediment transport.....	16
<b>4 Sea-floor sediments Southern Taranaki Bight – Hawera to Tangimoana</b> .....	<b>18</b>
4.1 Surficial sediments .....	20
4.2 Sediment bedforms and seabed morphology from side-scan sonographs.	21
4.3 Sub-surface sediments.....	23
<b>5 Ironsand Distribution</b> .....	<b>25</b>
5.1 Origin of offshore ironsand deposits .....	25
5.2 Surficial distribution .....	25
5.3 Sub-surface distribution.....	26
<b>6 Sub-surface geological structure</b> .....	<b>27</b>
<b>7 Aerial magnetic coverage for the South Taranaki Bight</b> .....	<b>30</b>
7.1 Background.....	30
7.2 Analysis of archival aerial magnetic coverage and NIWA high-resolution 3.5 kHz seismic reflection profiles offshore of Patea .....	30
7.3 Fugro aerial magnetic survey 2010-11 .....	33
<b>8 Summary of recommendations arising from 2009 report</b> .....	<b>36</b>
<b>9 Bibliography</b> .....	<b>37</b>
<b>Appendix A NIWA archive sediment samples</b> .....	<b>42</b>

<b>Appendix B</b>	<b>NZOI 1:200,000 Coastal Sediment Chart Series .....</b>	<b>42</b>
<b>Appendix C</b>	<b>3.5 kHz seismic acoustic facies maps with sediment sample locations .....</b>	<b>42</b>
<b>Appendix D</b>	<b>Ironsand concentrations and distribution .....</b>	<b>42</b>
<b>Appendix E</b>	<b>Compilation of archival aerial magnetic coverage and high-resolution 3.5 kHz seismic reflection profiles, Patea.....</b>	<b>42</b>
<b>Appendix F</b>	<b>Reduced-To-Pole 1<sup>st</sup>-Vertical Derivative magnetic coverage from Fugro aerial magnetic survey with unpublished NIWA fault data.....</b>	<b>42</b>

## Tables

Table 2-1:	Research and commercial surveys undertaken in the North and South Taranaki bight areas by NIWA (and its predecessor New Zealand Oceanographic Institute) from 1950 to prior to the commencement of prospecting by TTR.	14
Table 4-1:	Generalized seismic-sediment facies for the North and South Taranaki bights determined from high-resolution 3.5 kHz seismic reflection data.	20
Table 5-1:	Statistics for each of the five mining areas identified by TTR.	27

## Figures

Figure 1-1:	Map of active minerals permits for the North Island of New Zealand (from the NZPM website, Aug 2013). The dashed blue line is the 12 NM limit. (Data and image modified from NZPM permits portal). TTR's mining permit application relates only to sub-areas within 55581.	9
Figure 2-1:	Non-NIWA surveys (grey lines) and NIWA geophysical surveys (black lines) for the west coast, North Island. The stippled areas outline TTR's original prospecting permit areas PP 50383 and 50753.	12
Figure 3-1:	Map from Lewis (1979) of the generalised littoral sand-transport paths for black ironsand (chequered) and quartz-rich, light-coloured sand (fine stipple).	18
Figure 4-1:	A diagrammatic summary of bedforms by Lewis (1979) determined from side-scan and high-resolution seismic reflection surveys.	22
Figure 6-1:	Boomer profile across the shore-attached sediment wedge off the northern Manawatu coast from Nodder et al. (2007).	28
Figure 6-2:	Boomer seismic profile from Nodder et al. (2007) showing a broad seafloor scarp and thick synsedimentary wedge.	28
Figure 7-1:	Boomer seismic profile on the mid-shelf off Patea showing small fault splays and active tectonic deformation in the hanging wall of the Taranaki Fault, and thick synsedimentary deposits along the footwalls of the splays.	33
Figure 7-2:	Schematic representation the shelf depositional system on the South Taranaki Bight: (A) <6,500 years ago, and (B) lowstand conditions during the last-glacial maximum ~18,000 years ago. Figure from Feijth and Lowe (2011).	35

Reviewed by

A handwritten signature in blue ink, appearing to read 'S. Nodder', with a horizontal line underneath.

Dr Scott Nodder

Approved for release by

A handwritten signature in blue ink, appearing to read 'A. Laing', with a horizontal line underneath.

Dr Andrew Laing

## Executive summary

A fifty-year archive exists at NIWA, comprising limited sediment samples, cores, and coverage by seismic reflection and side-scan sonar surveys in the South Taranaki Bight. Here, a shore-connected Holocene sand prism, up to 20 m in thickness at the coast, extends seaward to around 20-30 m water depth. At its feather edge, the prism thins onto a transgressive erosion surface, delineated by coarse-grained lag deposits. The middle shelf is also covered by a sheet of gravel and sand, is commonly rippled by wave action, and is draped with 1-3 m of muddy sediment at > 50 m water depth. At around 100 m water depth, muddy deposits dominate the seabed and sub-seafloor. While this basic architecture applies regionally, the South Taranaki and Wanganui bights exhibit structural and sedimentological complexity.

Potentially thick deposits of ironsand occur in the shore-attached sand prism, in post-glacial bedforms and strandlines, and infilling fault-controlled sedimentary depocentres with kilometres of lateral extent along strike where they intersected the littoral transport path or trapped fluvial channel deposits. Sediments containing >5% ironsand are largely spatially restricted to the inner and middle shelves. On the middle shelf, buried, coarse-grained transgressive deposits that occur south of Patea and Wanganui could contain ironsand concentrations.

The limited suite of intact shelf cores archived at NIWA show that measured iron concentrations are variable, but typically increase down-core with a relative enrichment of ironsand in the shell gravel lag at the base. This trend appears to be less apparent nearer the shore, perhaps reflecting wave resuspension and reworking of sediments during the latter stages of the marine transgression or highstand during the Holocene.

An integrated analysis of aerial magnetic surveys off Patea (supplied by TTR) and NIWA seismic reflection data was inconclusive. In plan form, the sinuous magnetic anomalies are geometrically similar to a meandering river channel, whilst linear features have geometries of coarse-grained bars or exposed bedrock ridges. A review of NIWA's high-resolution 3.5 kHz profiles indicates that magnetic anomalies can coincide with some sub-surface reflectors, but appear inconsistent with near-seabed geometries (top few metres) and seismic echo-character. Recent boomer surveys contracted by TTR, together with results from their extensive drilling campaign, now form a valuable dataset to test the sub-seafloor occurrence and geometry of the meandering channel-fill complexes inferred from the aerial magnetics.

Sediment supply, lowstand alluvial channel systems and glacio-eustatic sea-level were undoubtedly important controls on the development of the South Taranaki Bight shelf depositional system. Throughout glacio-eustatic cycles, the relative position of the paleo-shoreline would have controlled sediment dispersal and depositional processes, and in turn many of the magnetic anomalies are inferred to have had a geomorphic origin. However, the geomorphic evolution, preservation potential, and sediment sources of some of these deposits, notably the paleo-river channel systems and dunes remain speculative.

Despite many uncertainties, aerial magnetic anomalies have made a significant contribution to the development of the resource assessment, by enabling TTR to characterise large areas of their tenements and discriminate areas with potentially high concentrations of ironsand. This underpinning dataset provided targets for coring campaigns that followed, and yielded baseline information that can be readily tested and complemented with other field data and resource models.

Information relating to TTR's additional scientific work undertaken since 2014 has been provided and the conclusions in this report remain valid.

# 1 Overview

Ironsands are the largest known reserve of metalliferous ore in New Zealand. Ironsand is a general term for sand-sized grains of iron-rich minerals, principally magnetite ( $\text{Fe}_3\text{O}_4$ ), titanomagnetite ( $\text{Fe}_2\text{TiO}_3$ ), and ilmenite ( $\text{FeTiO}_3$ ). New Zealand's ironsands occur extensively in coastal dunes and on the adjacent continental shelf of the western North Island, and have been successfully mined onshore for over 35 years (e.g. Mauk et al., 2006).

Offshore deposits of ironsand have been known since the early 1960's (e.g. McDougall, 1961), but estimates of their reserves are poorly constrained (e.g. Carter, 1980) and to date remain unexploited. With the growing demand for raw materials on international markets, there has been increasing interest in the feasibility of exploiting beach, shoreface and submarine ironsand deposits. Since 2005, there has been significant interest in offshore prospecting permits in New Zealand. Geographically, these active and applied permits cover almost the entire west coast of the North Island north of the Wanganui Bight (Figure 1-1). In addition to Trans-Tasman Resources Ltd (TTR), other mining companies that have also initiated exploration programmes include Rio Tinto / Iron Ore New Zealand, Sinosteel Australia, FMG Pacific, Ironsands Offshore Mining, and Sericho Developments. Many have undertaken offshore sediment coring and drilling campaigns, aeromagnetic surveys, and marine geophysical surveys to better identify and quantify potential shelf and nearshore ironsand deposits.

## 1.1 Current ironsand mining

New Zealand's largest mines occur on land in coastal dune fields along the northern Taranaki coast, which locally form a strip a few kilometres wide (e.g. Stokes et al., 2006). Concentrations of titanomagnetite can locally reach 70% by weight in the youngest aeolian deposits and form the main ore resource. The largest ironsand mine at Taharoa opened in 1972, with 215 million tonnes of Proved and Probable Ore Reserves (as of 2002). Since then, New Zealand Steel Mining has provided continuous supply to its North Asian customer base, with peak annual exports of two million tonnes in the late 1970s. In 2008, 563,000 tonnes of ironsand had been mined from Taharoa. At the Waikato North Head mine, near the Waikato River mouth, figures published by Crown Minerals and New Zealand Steel Ltd indicate that 1.160 million tonnes of sand were mined in 2008. The deposit reportedly contains around 107 million tonnes of Proved and Probable Ore Reserves (as of 2004).

The Waikato North Head and the Taharoa mines occur in large basement depressions that have provided significant accommodation space to develop thick ironsand deposits. The former occurs in a subsided graben (fault-bounded valley) immediately north of the Waikato River, and the latter partly infills a river valley (Mauk et al., 2006).

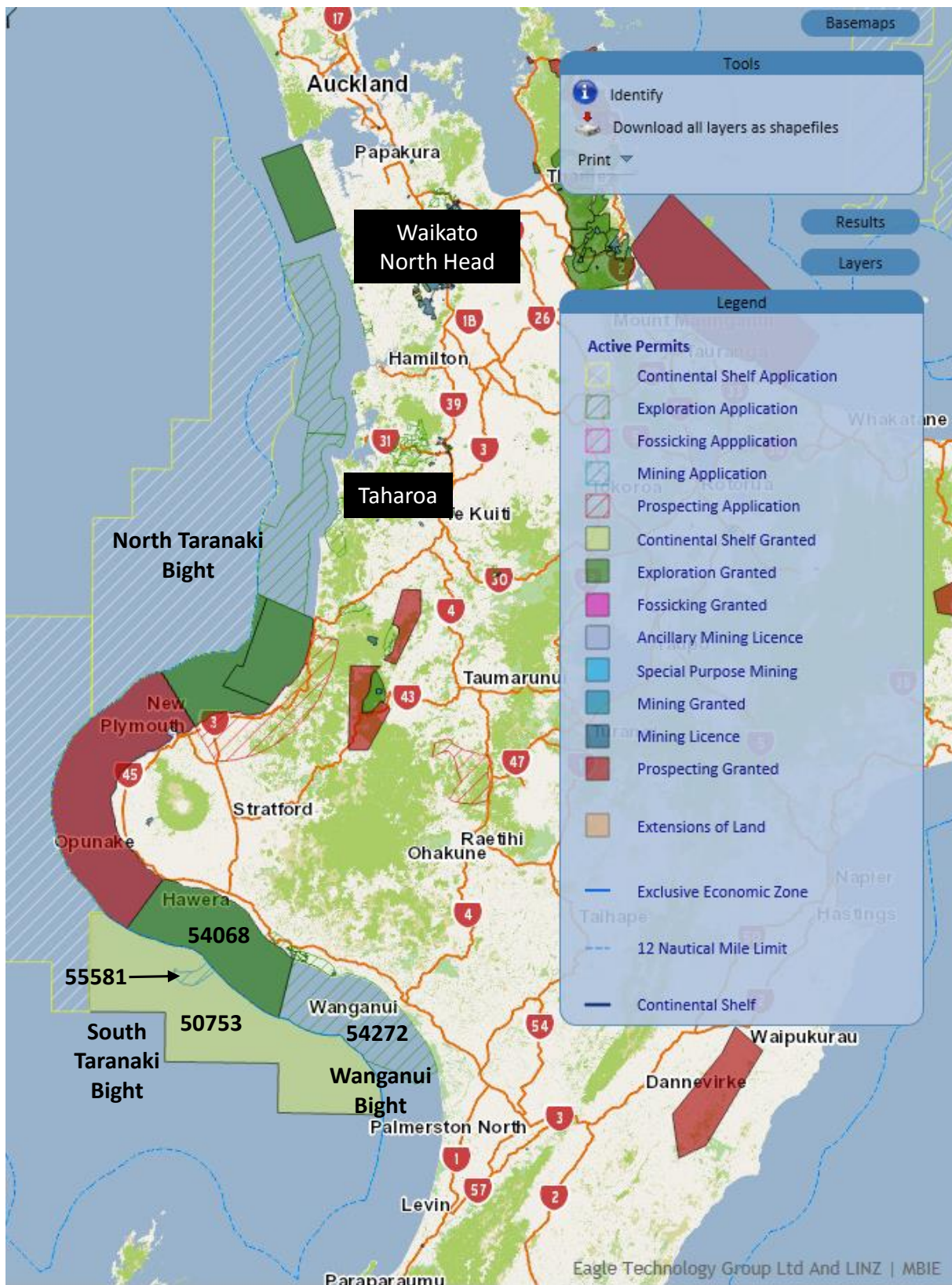


Figure 1-1: Map of active minerals permits for the North Island of New Zealand (from the NZPM website, Aug 2013). The dashed blue line is the 12 NM limit. (Data and image modified from NZPM permits portal). TTR's mining permit application relates only to sub-areas within 55581.

## 1.2 Scope of work

Trans-Tasman Resources initially secured a permit in early 2008 (PP 50383) to commence prospecting for offshore ironsands along the west coast, North Island, within the 12 nautical mile (NM) territorial sea, along the southern and northern Taranaki bights (Figure 1). The total area of PP 50383 was 6319 km<sup>2</sup>. A second exploration permit beyond the 12 NM territorial sea (PP 50783) was granted for the South Taranaki Bight, which was 2284 km<sup>2</sup> in area. Subsequent coring campaigns since mid-2009, an aerial magnetic survey, and marine geophysical surveys yielded further information to aid identification and quantification of a potential ironsand resource and the environment. As of August 2013, TTR progressed their survey and development programme to have two active exploration permits (54068 and 50753), an exploration application (54272), and a mining application (55581) in the South Taranaki Bight. The submitted licence area (beyond the 12 NM territorial sea) will be managed by the Environmental Protection Agency (EPA) under the new Exclusive Economic Zone and Continental Shelf (Environmental Effects) Act 2012. In the current application, TTR is seeking marine consents only in relation to those areas outside the 12 NM limit. Small sub-regions of interest within the mining application 55581 are “Xanthia”, “X2”, “Dianne” “D2” and “Christina”, which occupy a total extraction area of 53.6 km<sup>2</sup>. The area called “D2” is based on recent drilling results, which have highlighted that in some areas the ironsand resource is shallow and, with ongoing drilling, additional resource can be delineated within the mining area. Two active exploration permit applications by TTR remain for the North Taranaki Bight (54270 and 54271).

TTR contracted NIWA in mid-2009 to undertake an initial desktop study to assist ongoing prospecting and exploration within the permit areas (Orpin et al., 2009). This desktop report summarised the available geological and physical environmental data from published sources and NIWA’s fifty-year archive, comprising limited sediment samples, cores, and coverage by seismic reflection and side-scan sonar surveys. NIWA recommend that more cores were required to better constrain the three-dimensional variability in ironsand concentration, both within the shore-attached sand-prism and the buried, coarse-grained transgressive lags and post-glacial syndimentary deposits. The report also recommended that sub-surface information yielded from cores would complement and potentially ground-truth any new geophysical data.

## 1.3 Project brief

The current report provides a geological summary of the South Taranaki Bight area based on previously published material. It largely stems from NIWA’s previous geology desktop for TTR (Orpin et al., 2009), but also includes updated maps and references to be compatible with the current permit areas, recently acquired aerial magnetic survey (and report) and sediment/core samples collected by TTR since 2009. As specified in the original agreement, the following components are summarised:

- Overview, Scope of work, Project Brief, Data Discovery / Desktop Study.
- Compilation of data sources.
- Environmental setting relevant to the distribution of ironsand: ocean circulation; waves; sediment transport; littoral drift; and sediment migration.
- Seafloor sediments: surficial sediments; sub-surface sediments; sediment bedforms and seabed morphology from side-scan sonographs; and, sub-surface units from seismic reflection data.
- Ironsand distribution: surficial distribution and sub-surface distribution.
- Shallow, sub-surface geological structures.
- Comparison of aerial magnetic data (both archival and recently acquired from a Fugro survey for TTR) with known geological structures.

## 2 Data Discovery

NIWA holds considerable archival data relevant to the permit areas along much of North Island west coast, including bathymetry, geophysical data (Figure 2-1), and seafloor sediment and core samples, including data on grain size and mineralogy. Some of these data have been previously published (e.g. Carter, 1980). Data density is high for the South Taranaki Bight due to numerous industry site surveys and research voyages related to Maui gas field infrastructure, and eastern Wanganui Basin and Manawatu tectonics and sedimentology (Table 1; Nodder, 1990; Gillespie et al., 1998; Lamarche et al., 2005; Proust et al., 2005; Nodder et al, 2007). NIWA has undertaken other commercial consultancy projects during the late 1980's along the west coast, North Island. These include offshore surveys for submarine cable installations and sewer outfall off Manukau, submarine cable landings off Urenui and Waitoetoe Beach, and pipeline surveys associated with the Maui production platforms. All of these investigations have acquired closely-spaced, single-beam bathymetry, high-resolution seismic reflection data, seafloor side-scan mapping, and some limited seafloor photography and sediment sampling.

Specifically, the present report aims to: (1) review available published and unpublished geological interpretations for shelf and nearshore/coastal Quaternary sequences, with particular emphasis on the distribution and grade of ironsand deposits; (2) review knowledge of shelf and coastal shallow fault systems potentially relevant to the development of ironsand deposits; (3) review and present a synopsis of the broad Quaternary shelf sediment architecture; (4) within the constraints of the data, identify the geometry of the thickest ironsand deposits and their estimated volume; (5) provide an analysis of the aerial magnetic coverage (supplied by TTR) and existing NIWA seismic data offshore of Patea; and (6) identify areas of potential interest for future geophysical surveys and data needed to better constrain estimates of the ironsand resource.

### 2.1 Data sources

NIWA holds a considerable archive of data collected from research surveys extending back to the 1950's (Table 1). The equipment carried on the surveys varied considerably, and not until the advent of radar, Microfix, and then GPS, are navigation data entirely accurate.

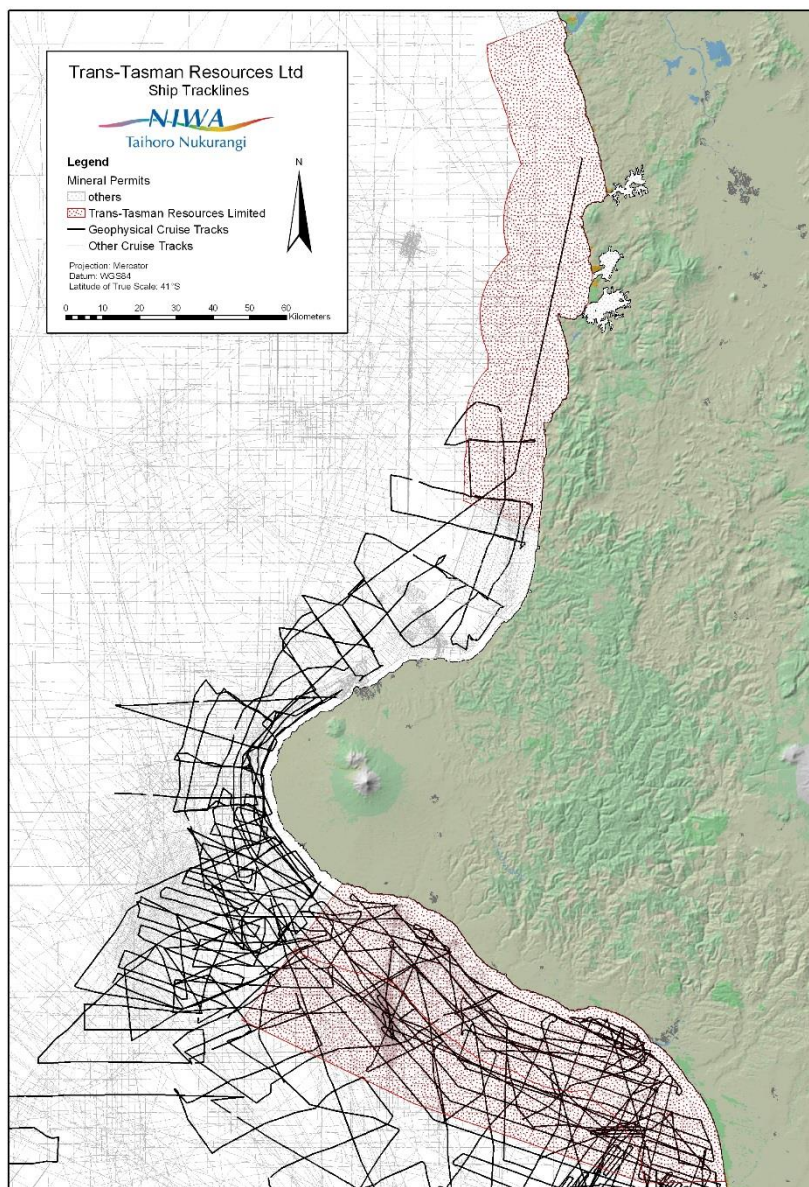


**Figure 2-1: Non-NIWA surveys (grey lines) and NIWA geophysical surveys (black lines) for the west coast, North Island. The stippled areas outline TTR's original prospecting permit areas PP 50383 and 50753.**

<b>NIWA Voyage Number</b>	<b>Year Collected</b>	<b>Data type</b>	<b>Navigation</b>	<b>Area</b>
	Nov-50	Sediment and core samples	No	NW North Is
450	Oct-58	Sediment and core samples	No	NW North Is
457	Sep-59	Sediment and core samples	No	NW North Is
464	Oct-59	Sediment and core samples	No	Manukau to Waitara
469	May-60	Sediment and core samples	No	NW North Is
505	Oct-62	Sediment samples	No	Manukau to Te Maika
511	Mar-63	Sediment samples	No	North Taranaki Bight
543	Nov-65	Sediment and core samples	No	NW North Is
597	Apr-70	Sediment and core samples	No	NW North Is
7040	Feb-72	Sediment samples	No	New Plymouth
CR1005	Jan-73	Sediment and core samples	Yes	NW North Is
CR1013	Jan-74	Sediment and core samples	Yes	NW North Is
CR1017	Feb-74	12 kHz	No	West Coast, Port Waikato
CR1025	Sep-74	Sediment samples	Yes	Cape Egmont
CR1027	Dec-74	3.5 kHz	No	NW North Is
CR1033	Mar-Apr 1975	3.5 kHz seismic and Sediment samples	Yes	Taranaki Bight
CR1043	Apr-May 1976	3.5 kHz seismic sediment and core samples	Yes	Taranaki Bight, Tirua Point
CR1036	May-75	Sediment and core samples	Yes	NW North Is
CR7048	Aug-75	Sediment sample	Yes	South of Raglan
CR1049	Sep-76	Sediment and core samples	Yes	NW North Is
CR1060	May-77	3.5 kHz	Yes	NW North Is
CR1065	Sep-77	Sediment and core samples	Yes	NW North Is
CR1077	Jul-78	Sediment and core samples	Yes	NW North Is
CR7086	May-80	Sediment samples	No	New Plymouth
CR1117	Jan-81	Sediment samples	No	Waitara

NIWA Voyage Number	Year Collected	Data type	Navigation	Area
CR2012	Sep-87	Sediment and core samples	Yes	North Taranaki Bight
CR2012	Sep-87	3.5 kHz seismic, Klein side-scan sonar, sediment and core samples	Yes	Cape Egmont, Taranaki Bight
CR7125	Mar-88	Sediment samples	No	Manukau
CR2031	Nov-89	3.5 kHz, sediment and core samples	Yes	NW North Is
CR2033	Mar-90	3.5 kHz, Klein side-scan sonar, sediment and core samples	Yes	South Taranaki Bight
CR2039	Oct-90	3.5 kHz, sediment and core samples	Yes	Taranaki Bight
CR2045	Jul-91	Sediment and core samples	Yes	NW North Is
CR2056	Jun-92	3.5 kHz, airgun, side-scan, sediment and core samples	Yes	Manawatu, South Taranaki Bight, Cape Egmont
CR3015	Oct-Nov 93	3.5 kHz	Yes	South Taranaki Bight, Manawatu
CR3048	Nov-98	3.5 kHz, airgun, sediment and core samples	Yes	South Taranaki Bight, Manawatu
TAN0105	Apr-May 01	3.5 kHz, boomer, sediment, airgun, and core samples	Yes	South Taranaki Bight, Manawatu
MD152	Jan 06	International research consortium, Matacore giant piston coring campaign	Yes	Manawatu

**Table 2-1: Research and commercial surveys undertaken in the North and South Taranaki bight areas by NIWA (and its predecessor New Zealand Oceanographic Institute) from 1950 to prior to the commencement of prospecting by TTR.**

## 3 Environmental setting

### 3.1 Ocean circulation

New Zealand sits in the eastward-flowing southern branch of the South Pacific subtropical gyre. This gyre is driven by the southeast trade winds to the north and the westerly winds to the south. These wind systems set up the anti-clockwise circulation within the subtropical gyre, which is also modified by the spin of the earth. The west coast of the North Island is presumed to block the eastward flows, and currents along the west coast of the North Island are generally weak, variable and unstructured at intra-annual timescales (Sutton and Bowen, 2011). The main current off the northwest coast of the North Island is called the West Auckland Current (WAUC), but the northwest coast of the North Island is one of the least investigated regions of New Zealand, with little oceanographic field data for the Taranaki region.

The continental shelf off the west coast of the North Island broadens to the south from a relatively narrow shelf about 20 km wide off Northland, to a broad shelf about 100 km wide at the North Taranaki Bight. The shelf narrows around Cape Egmont, then extends across the South Taranaki and Wanganui bights. The circulation on the shelf consists of three principal components:

1. Ocean-forced currents within the WAUC, travel south to southeast with weak flows speed of 3–8 cm/s west of Northland and Auckland (Sutton and Bowen, 2011). Inshore flows, in water depths <1000 m deep are complex, showing a transition between offshore and inshore fields, but with coastal measurements of mean northwestward flow of 2–4 cm/s, but with high temporal and tidal variability up to 10 cm/s. In the North Taranaki Bight, closer inshore current measurements show a mean along-shore current to the south, with mean velocities of ~6 cm/s recorded at 20 m water depth immediately north of Waitara from October 1983–November 1984 (Heath and Gilmour, 1987a; after data collected by the Taranaki Catchment Commission and Regional Water Board, 1985). The Westland and D'Urville currents are major low-velocity (mean speeds 1–10 cm/s), wind-driven oceanic flows that transport cold-water plumes and suspended sediment from the South Island into the southernmost portions of the South Taranaki and Wanganui shelves (e.g. Carter and Heath, 1975; Heath and Gilmour, 1987b; Harris, 1990).
2. On the Wanganui shelf, a southeasterly-directed, longshore littoral drift prevails, generated by the orientation of the predominantly west to southwest wave trains and the arcuate coastline between Taranaki and the Kapiti coast. Along the northern Manawatu coast, along-shelf currents can attain speeds up to 40 cm/s, but are likely to be of limited significance given the occasional exposure to high-energy storm waves (Perret, 1990; Dunbar and Barrett, 2005). This anticlockwise gyre around the embayment off Wanganui will be enhanced during strong westerly storms.

3. The largest and principal tidal component on the New Zealand coast is the lunar and semi-diurnal tide (M2) with a period of 12.42 hours. This M2 tide consists of a progressive wave that propagates anticlockwise around New Zealand, and a standing wave on the west coast of New Zealand (Heath, 1982). Normal tidal currents on the Taranaki continental shelf have speeds around 7 cm/s, and internal tides may generate flows up to 30 cm/s at the shelf edge. Although swift tidal flows can exceed 125 cm/s through the Cook Strait Narrows region, they are significantly weaker at <25 cm/s over the Wanganui shelf (Proctor and Carter, 1989).

### 3.2 Waves

A Hindcast wave model, based on 20 years of regional wind pattern data, indicates that the simulated wave climate for the Cape Egmont region for the near-shore (<30 m) has a mean significant wave height of 1.97 m, but with significant wave heights >3 m and >5 m occurring 10 % and 0.55 % of the time, respectively (summarised in Gorman et al., 2003). The mean wave period is 6.97 s, with a mean wave direction from the west-southwest. The wave climate at Maui-A production platform, off Cape Egmont, is also strongly seasonal with two distinct periods: a more quiescent wave climate over the summer (Dec-May); and more vigorous waves over winter (Jun-Nov) (Ewans, 1998; Ewans and Kibblewhite, 1990; Kibblewhite et al., 1982). The highest waves recorded at Maui-A reach approximately 20 m during the winter (Kibblewhite et al., 1982).

Wave-rider buoy data from Buxton et al. (1986) suggests that at 40 m water depth at the Te Ranga-A drill-site, in the North Taranaki Bight, the wave energy is lower than at Maui-A. Pickrill (1987) suggests that this might be due to: (1) shallower water; and (2) wave energy that generally increases southward along the west coast of New Zealand (cf. Pickrill and Mitchell, 1979; Gorman et al., 2003).

Wave-rider data from Macky et al. (1988) show a decrease in the significant wave height and energy eastward from around 110 m the Maui-A production platform to a wave height of 1.3 m on the Wanganui shelf.

### 3.3 Sediment transport

Along the North Taranaki Bight, tidal and mean flows are too weak to transport sediment (Carter and Heath, 1975). The majority of sediment transport will occur during storms (Lewis, 1979; Carter, 1980), when winds can exceed 100 km/h. The prevailing westerly and southeasterly winds can also generate wind-drift currents with speeds of 27 cm/s and 15 cm/s in water depths of 30 m and 75 m, respectively (Carter, 1987). High winds generate a vigorous wave climate with sufficient energy to resuspend sand-sized particles, which could then be entrained in wind-generated currents. Over 75% of the recorded waves along the west coast of the North Island have wave heights of 1-3 m and periods of 6-8 s (Pickrill and Mitchell, 1979), which is sufficient to resuspend the fine sand and mud on the seabed down to 40 m. On the easternmost Wanganui - north Manawatu shelf, under normal wave conditions (significant wave height of 0.5 m and period of 7 s; Perrett, 1990), an analysis of bed shear stress by Dunbar and Barrett (2005) suggest that mud resuspension occurs regularly to ~15 m water depth. During extreme waves, Carter (1987) suggests seabed stirring may occur down to 150 m water depth, during which time sediments on the inner shelf will be in a state of constant movement, a conclusion supported by the well sorted nature of the inner shelf sands.

Secondary flows, such as storm induced bottom-return currents, may also occur in response to exceptional weather patterns. Lewis (1979), for example, calculates that a storm-surge current with near-bed current speeds of 60 cm/s was formed in the South Taranaki Bight during an extremely large westerly storm in 1976. Lewis concluded that extreme events will likely generate currents sufficient to mobilise sand ribbons and ridges off Wanganui (Lewis, 1979). Bottom photographs described by Lewis (1979) indicated evidence of the progressive degradation of ripples and megaripples by superposition of younger bedforms.

The black ironsands found along this coastline are primarily sourced from poorly consolidated, Mt Taranaki andesitic volcanic lahar deposits of late Quaternary age that outcrop in coastal cliffs and stream banks (Fleming, 1946; Matthews, 1979; Gibb, 1978, 1979).

Quantification of littoral sediment transport is poorly constrained by observational data for the North Island west coast in general. Early studies suggest that there is a general decrease in the concentration of dense, natural ironsand away from sources derived from Mt Taranaki/Egmont, particularly evident on the north of Cape Egmont (Nicholson and Fyfe, 1958; Kear, 1965; Carter, 1980). Pickrill (1987) suggests that, immediately following construction of the Port of New Plymouth at the turn of the century, sediment built up on the southern side of breakwater, while there was net sediment erosion on the northern side. Based on field evidence of Blair (1890, reprinted in 1968), an estimated 580 000 m<sup>3</sup> of sediment accumulated over a 7 year period after construction (approximately 8000 m<sup>3</sup>/yr). Matthews (1977), however, estimated that the net littoral drift from Cape Egmont to New Plymouth was much higher, around 75,000 to 180,000 m<sup>3</sup>/yr. In contrast, Pickrill (1987) suggests that around the New Plymouth area the sediment budget shows net sediment loss, and that the quantities of sand in longshore transport are considerably less than in other comparable high-energy, exposed ocean shores around New Zealand.

Lewis (1979) describes modern and ancient along-shore transport to the southeast for Taranaki-sourced ironsand in the Wanganui Bight area. Ironsand-rich sand ridges occur on the inner and mid-shelf (Figure 3-1). Present-day ironsand dispersal paths are along the beach face, with quartz-sands derived directly from out of the river mouths. In contrast, off Patea ironsand deposits are dammed by rock outcrops (solid black in Figure 3-1) during the last phase of the sea transgression (around 7,000–9,000 years ago). Further seaward, the broken stippled-belt in Figure 3-1 shows an uninterrupted longshore drift of ironsand, inferred to have occurred during an even earlier phase of the transgression around 9,000–12,000 years ago. Modern ironsand deposits remain largely at the shoreface, within the coastal littoral zone, helping to prograde beaches southeast of Wanganui, or material is blown inland to form aeolian sand dunes. However, a small fraction of the ironsand and felsic-sand component escapes the surf zone and helps build out the smooth shoreface to a depth of about 15 m (Figure 3-1)

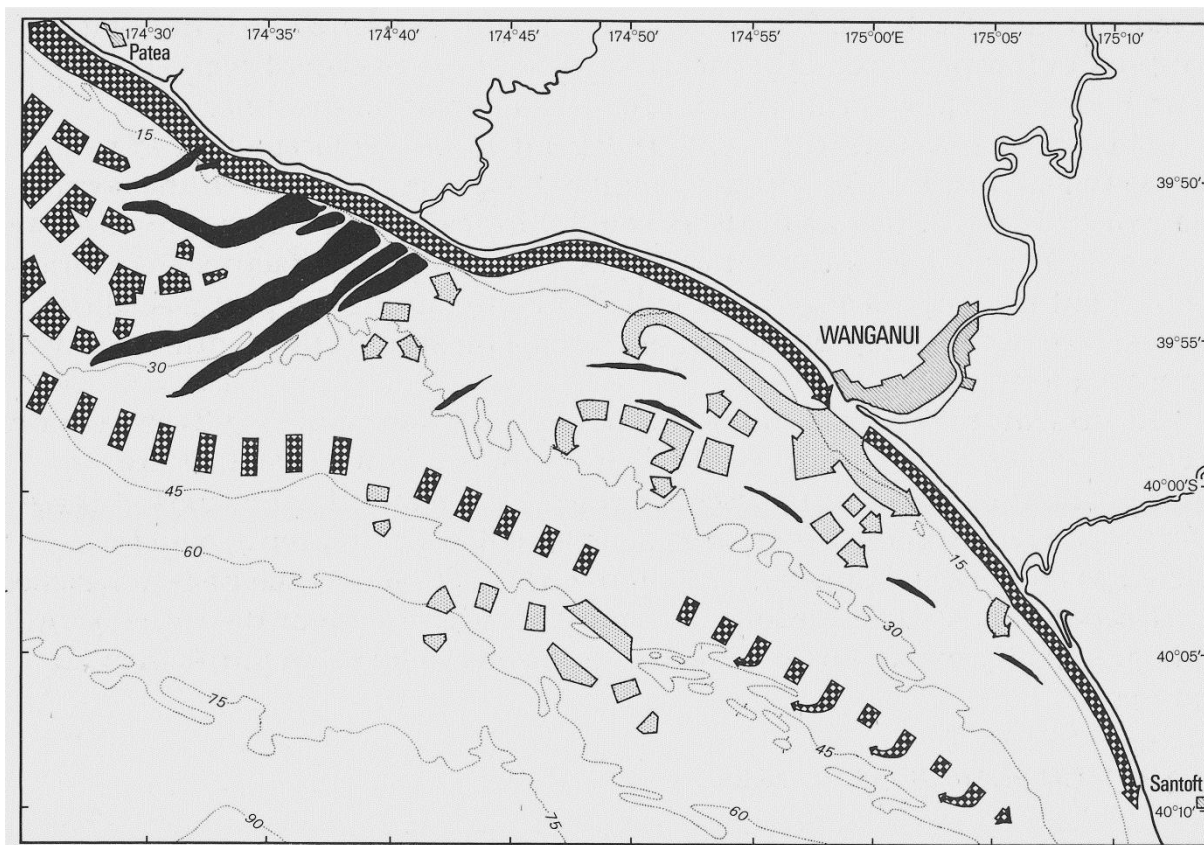
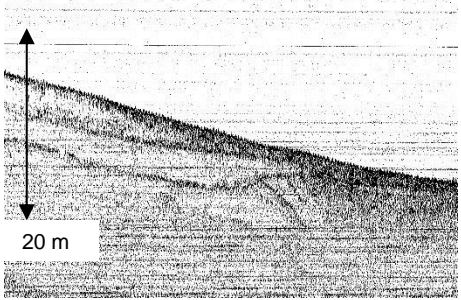
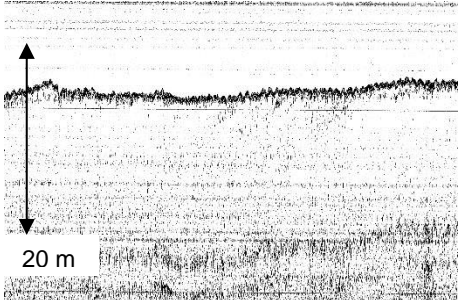
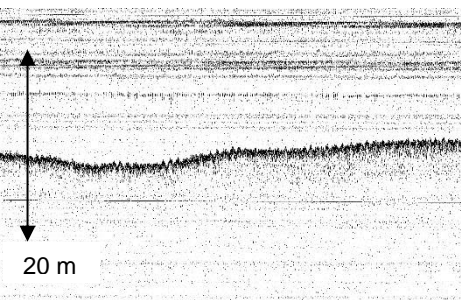
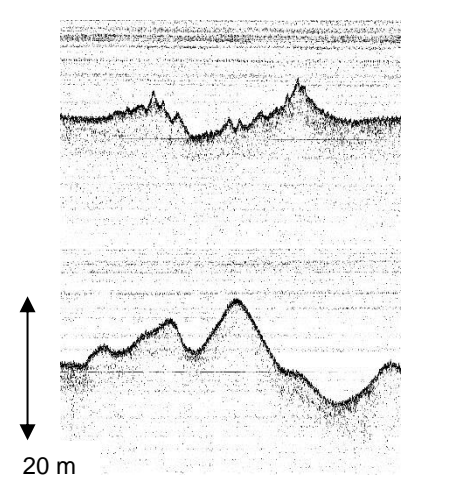


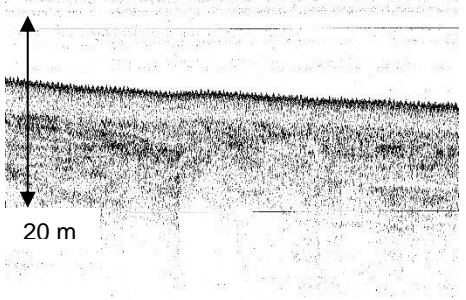
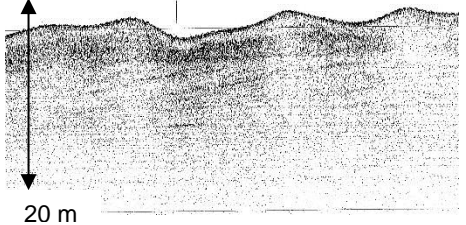
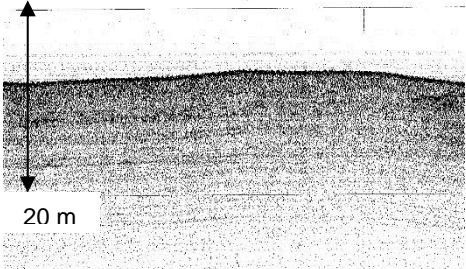
Figure 3-1: Map from Lewis (1979) of the generalised littoral sand-transport paths for black ironsand (chequered) and quartz-rich, light-coloured sand (fine stipple).

#### 4 Sea-floor sediments Southern Taranaki Bight – Hawera to Tangimoana

The patterns of sediment deposition that have characterised seafloor of the South Taranaki and Wanganui bights since the last-glacial maximum were controlled primarily by glacio-eustatic sea-level rise. Other contributing drivers were the quantity and lithology of terrigenous sediment supply and the evolving hydraulic regime of the shelf, from initially tide-dominated to storm-dominated as sea level rose and Cook Strait opened (Gillespie et al., 1998). The last glaciation reached its maximum in New Zealand approximately 18,000 years ago (Pillans et al., 1993), when sea level was about 120 m lower than today (Carter et al., 1986). The subsequent post-glacial sea-level rise occurred episodically, as a series of rapid transgressions punctuated by stillstands, or even minor regressions, which lasted up to two thousand years in (Carter et al., 1986). Modern sea level ( $\pm 1$  m) was attained  $\sim 6,500$  years ago (Gibb, 1986; Pillans, 1990).

Sediment samples from grabs and cores from the NIWA archive are compiled in Appendix A. The sample descriptions include both field and laboratory notes. Acoustic responses, sub-surface geometry and stratigraphic relationships yielded from 3.5 kHz, high-resolution seismic-reflection surveys from the permit areas are summarised and compiled as acoustic facies in Table 4-1 and spatially depicted in Appendix C, following the methodology of Damuth (1980) for characterising seabed and sub-seafloor echo-types.

Echo facies	Echo Character	Interpretation	Example
Shore-attached, muddy fine-sand	Strong, sharp seafloor reflector with underlying transparent to diffuse unit containing weak to wavy internal reflectors	Active coastal sediment wedge prograding out from shoreline, nourished by littoral transport of modern riverine sediment output and reworking of coastal dune deposits	
Bedrock with thin veneer of sandy gravel	Strong, irregular, sharp bottom reflector, slightly prolonged in places where a patchy thin (<1 m) veneer, underlain by weak dipping reflectors that are truncated at the seafloor.	Patchy, thin veneer of modern and relict shelly gravel at the seaward feather edge of the modern coastal sediment wedge, overlying eroded wave-cut platform of mudstone.	
Strongly reflective gravelly sand	Strong, sharp bottom reflector underlain by very diffuse or no reflectors.	Condensed, gravelly-sand sheet of modern, transgressive, and palimpsest shelly lags.	
Coarse sand with dunes and megaripples	Strong, sharp bottom reflector, pronounced surface topography (up to 7 m) with symmetrical and asymmetrical dunes and megaripples.	Condensed, gravelly-sand sheet of modern, transgressive, and palimpsest shelly lags. The large dunes likely formed during the transgression and the megaripples from recent storms.	

Echo facies	Echo Character	Interpretation	Example
Gravelly/sandy mud, 1-3 m thick	Strong, slightly prolonged bottom reflector, underlain by a transparent unit, 1-3 m in thickness, with a diffuse prolonged reflector at its base that has irregular, discontinuous internal reflectors.	A thin but extensive Holocene mid-shelf mud deposit containing palimpsest shell and sand, overlying a channelised post-glacial transgressive erosion surface and coarse-grained condensed section.	
Gravelly/sandy mud drape over relict dunes	Undulating, strong, bottom reflector, underlain by a transparent unit, 1-3 m in thickness, which drapes over an undulating diffuse prolonged reflector, sometimes with weak internal reflectors.	A thin but extensive Holocene mid-shelf mud deposit with a coarse carbonate and sand component, draping over coarse-grained, transgressive dunes.	
Outer shelf muddy deposit	Moderately strong, prolonged reflector, underlain by stacked weak sub-horizontal reflectors.	Fine-grained modern outer-shelf sediment, underlain by laminated transgressive and lowstand deposits.	

**Table 4-1: Generalized seismic-sediment facies for the North and South Taranaki bights determined from high-resolution 3.5 kHz seismic reflection data.**

## 4.1 Surficial sediments

The regional surficial sediment character of the southern permit area is captured in two published 1:200,000 Coastal Chart Series New Zealand Oceanographic Institute charts (Appendix B): Patea Sediments for the majority of the area south of Cape Egmont (Nodder et al., 1992), and the northernmost extent of Cook Strait Sediments for the southeastern extent of the permit area (Lewis and Mitchell, 1980). These maps summarise the textural and compositional character of the sea floor, based upon sea bed samples and interpolation between samples.

The Patea surficial sediment map indicates that the continental shelf from the South Taranaki Bight to Wanganui Bight is complex, and more heterogeneous than the northern permit area. Here, shoals affect shelf gradients, namely the Patea and Graham banks, and The Rolling Ground. The inner and mid-shelf gradient steepens to the south, entering the northern approaches of Cook Strait. Unlike the northern permit area, shells and shell hash are plentiful, and a coarse carbonate gravel component is ubiquitous southeast of the South Taranaki Bight and west of the Farewell Rise.

The inner and mid-shelf shoals are predominantly gravel sands, rich in shell material, with The Rolling Ground and Patea Bank comprising >50% carbonate. Graham Bank is a coarser grained, carbonate-rich (>50%) sandy gravel. Sandy sediments dominate to >100 m water depth on the low gradient, wide shelf offshore of Hawera. Sandy sediments also occur as a shore-connected belt around 12-15 km wide that follows the coast. Silt and mud fractions (<50%) occur in a band up to 5 km wide between the mouths of the Waitotara and Whangaehu rivers with a sandy silt lobe centred around the Wanganui River. Away from the coast, finer-grained silt deposits occur seaward of the 80 m isobath on the Wanganui Bight, where inner and mid-shelf gradients are steeper and at northern extent of the Manawatu mud belt (Nodder et al., 1992).

## **4.2 Sediment bedforms and seabed morphology from side-scan sonographs**

A range of bedforms have been described from the Wanganui Bight area, ranging in size, mineralogy, and origin. Side-scan sonar data described by Lewis (1979) and Nodder (1990) form the basis for the detailed knowledge of bedform morphology, in concert with supporting seismic reflection data summarised by Lamarche et al. (2005) and Nodder et al. (2007).

According to Lewis (1979), bedforms determined from side-scan and high-resolution seismic surveys form two basic types: (1) those in the nearshore zone are mainly erosional; and (2) those offshore are depositional. Erosional bedforms occur at <30 m water depth, and include rock outcrops and ancient buried river valleys formed by the differential weathering of the underlying Plio-Pleistocene mudstone. In contrast, at >30 m water depth storm-generated depositional bedforms occur, including ironsand ridges, sand ribbons, symmetrical megaripples and sand waves (Figure 4-1). Bedforms that occur close to shore within the stippled belt shown in Figure 4-1 were interpreted to be erosional. These include rock outcrops (heavy broken lines) and ancient buried river valleys (line of V's). In contrast, seaward of the stippled zone, the bedforms were interpreted to be depositional, generated by storms. These include ironsand ridges (grey dense stipple; also summarised in Carter, 1980), sand ribbons (bold lines), symmetrical megaripples (fine lines), and sand waves (arrowed lines). The inset in Figure 4-1 shows the direction of large waves stirring fine sand at 30 m (white fill) and 50 m (solid black fill). The wave orientation is dominantly west-southwest. The largest sediment bodies are situated immediately southeast of the mouth of the Wanganui River (Figure 4-1). These deposits are 4-12 m high, several hundred metres wide and several kilometres long, aligned sub-parallel to the coastline. Their surface is composed of ironsand and volcanic pebbles, interpreted to be sourced from Mt Taranaki. These sand ridges are located on relatively flat seafloor (Lewis 1979).

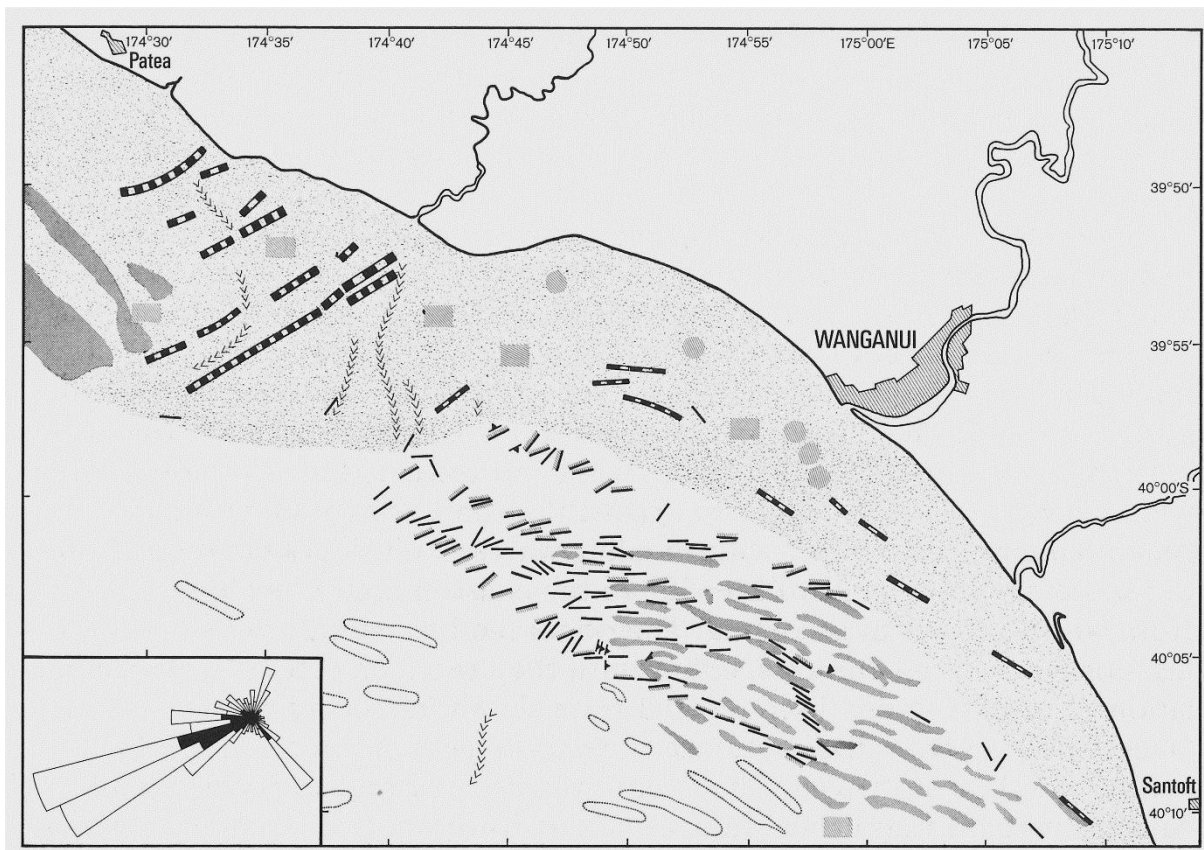


**Figure 4-1: A diagrammatic summary of bedforms by Lewis (1979) determined from side-scan and high-resolution seismic reflection surveys.**

An analysis by Lewis (1979) of the hydrodynamic motions required to create bedforms of this size at 30–50 m water depth inferred that they are more likely to be formed 9,000–12,000 years ago as shore-connected shoals. Their location and orientation on the shelf is consistent with the estimated position of the transgressive shoreline (Proctor and Carter, 1989; Lewis, 1994). Lewis (1979) infers that their formation ceased about 9,000 years ago with rising sea level, when Plio-Pleistocene rock promontories around 25 km west of Wanganui began to act as natural barriers to the supply of ironsand within the littoral drift system. As the sea transgressed the inner shelf, these outcrops of semi-indurated shelly sandstone and siltstone formed headlands and reefs that dammed the eastward, longshore supply of ironsand. Supply was not re-initiated until present-day sea level was attained ~6,500 years ago and headlands were eroded back to allow longshore drift to develop once again. Ironsand shoals of similar size and morphology have not been described on the modern shoreface.

Within the intervening troughs, between large ironsand ridges, are a complex array of smaller active bedforms, including sand ribbons, ripples (0.1–0.5 m wavelength), symmetrical megaripples (1–3 m wavelength) and sand waves (Figure 4-1). These bedforms persist to depths of >50 m water depth, and were presumably formed by strong oscillatory currents, approaching 1 m/s, which occur during the passage of large storms (Lewis, 1979).

Sand ridges and dunes, 3–12 m in height (Table 4-1), occur in two large zones around 100 km<sup>2</sup> in area off Wanganui (cf. Lewis, 1979), and as isolated patches <20 km<sup>2</sup> in the vicinity of The Rolling Ground off Patea (Appendix C). Data collected during NIWA voyage CR2033

(Nodder, 1990) indicates that the bottom topography is a series of northwest-southeast trending, submarine ridges and troughs, composed of coarse sand-gravel, but with a thin, patchy veneer of fine sand. Similar to the ironsand ridges observed off Patea by Lewis (1979), the coarse deposits are believed to have formed during the last phase of the sea level transgression around 8,000–10,000 years ago, whereas the fine-sand cover is probably a modern deposit at the seaward edge of the shore-attached sediment prism.

The analysis of bottom photographs and side-scan imagery by Lewis (1979) and Nodder (1990) indicate that the seabed is undergoing constant modification, and the exact location or spatial extent of bedforms, particularly small scale features such as sand ripples and ribbons, are likely to change with time.

### 4.3 Sub-surface sediments

The near-surface sedimentary units (top 20 m) from the Wanganui Bight region have undergone significant exploration using a range of acoustic equipment, including high-resolution 3.5 kHz, boomer and multichannel seismic systems (e.g. Nodder, 1990; Gillespie et al., 1998; Lamarche et al., 2005; Proust et al., 2005, Nodder et al., 2007). In addition, a number of cores and bottom samples have been collected and published (e.g. Nodder, 1993; Gillespie et al., 1998; Nodder et al., 2007).

In general, the sediment facies show a seaward succession of facies (cf. Gillespie et al., 1998). At the coast, a shoreface-attached sandy deposit, several metres thick, downlaps onto thin, condensed, coarse-grained sands and gravels sheets on the mid-shelf. Muddy deposits are better developed at >50 m water depth, typical of this wave-graded coastline where mud content broadly increases seaward as a function of wave energy (Dunbar and Barrett, 2005). At around 100 m water depth, well-developed stacked reflectors mark the development of a thick muddy deposit; that is, modern outer-shelf mud overlying lowstand and transgressive deposits (Table 2-1). Despite high rates of sediment supply regionally from rivers, the Wanganui mid-shelf itself has been relatively starved of terrigenous sediment, and widespread shelly-gravel lags have been able to accumulate on the central shelf over the last 12 000 years, since the early phase of the last-glacial sea-level rise (Gillespie et al., 1998).

The modern, shore-attached sandy prism is well developed throughout the Wanganui Bight, but particularly at the southeastern margin of the permit area, offshore of Tangimoana. Here, the deposit widens slightly to 6 km (around 40-50 m water depth) and shows considerable thickness variations locally, associated with faults that have actively displaced underlying Quaternary deposits (discussed further in Section 7 below). Maximum thickness attains 22 m locally, but more generally measured seismic thicknesses are 5-6 m. The sandy prism tapers seawards and downlaps onto the condensed, coarse-grained mid-shelf sheet deposits at around 20-30 m water depth.

Offshore of Patea, the lateral transition is more complex, influenced by emergent semi-indurated Plio-Pleistocene sedimentary rocks along the north-south trending basement structure of the Patea-Tongaporutu High (e.g. Anderton, 1981) in the vicinity of The Rolling Ground, Patea and Graham banks, the North and South traps, and east towards Wanganui (Appendix B). Evidence of eroded and truncated bedrock is seen in high-resolution 3.5 kHz sections (Table 4-1), consistent with earlier 3.5 kHz and side-scan surveys described by

Lewis (1979) and Nodder (1990). Here, only a patchy thin veneer (<1 m) of coarse gravelly sand covers the eroded bedrock.

Two mid-shelf deposits are recognised: (1) a condensed, gravelly sand sheet; and (2) a gravelly/sandy mud drape of 1–3 m in thickness, overlying a strongly reflective condensed unit (Table 4-1). Cores from the Manawatu coast, south of the permit area, suggest that the age of this regionally extensive transgressive surface is 10,000–11,000 years old and is composed of a coarse-sandy lag (Nodder et al., 2007). The gravelly/sandy mud seismic facies generally occurs seaward of the 50 m isobath and the gravelly sand sheet, except for a narrow, coast-parallel tongue that extends eastwards from the western boundary of the permit area in the South Taranaki Bight.

Seismic sections provide compelling evidence for younger muddy deposits draping over older buried sand ridges, consistent with the findings of Gillespie et al. (1998). The buried dune fields occur in two large areas, up to 400 km<sup>2</sup> lateral extent south of Patea and Wanganui (Appendix C). The underlying dunes appear as prolonged, weak to irregularly stacked reflectors, suggesting that they are condensed, coarse-grained deposits, similar to the exposed sand ridges observed close to the coast off Wanganui (cf. Lewis, 1979). In the absence of any age control, the origin of these earlier deposits is not clear, but they could have formed during a sea-level stillstand early in the last-glacial transgression. Moreover, their mineralogical composition can only be speculated, but could well contain shell, gravel, felsic sand and mafic/ironsand components.

By way of a comparison to other published depositional models for the Taranaki shelf over multiple sea-level cycles, the stratigraphic position of sand deposits and channels over the Plio-Pleistocene and Quaternary has been fundamentally linked to glacio-eustatic sea level cycles. Nodder (1995) examined offshore late Quaternary transgressive/regressive sand sequences, interpreted from seismic reflection profiles (3.5 kHz, airgun), and piston core and borehole stratigraphic logs, collected from mid-outer shelf depths (50-130 m) on the Taranaki continental shelf. Here, high amplitude seismic units, characterised by erosive, channelised bases in the vicinity of the Farewell Rise, were inferred to represent transgressive nearshore deposits that developed under rising sealevel conditions, rather than glacial lowstand sequences. The erosive unconformities at the bases of these units were probably developed during the peak of sea-level lowstand. High-amplitude channel-fill seismic units were inferred to be possibly fluvial and/or near-shore sediments, deposited during the sea-level lowstand and/or the ensuing transgression.

Estimating the volumes of these seismic facies to aid potential resource estimates is problematic given the complex surface and sub-surface morphology. Nonetheless, given the seismic survey data available, Orpin et al. (2009) suggested that sandy postglacial units >5m thickness were likely limited to the following deposits: (1) the modern shore-attached sand wedge along the landward boundary of the permit; (2) relict sand ridges and dunes off Wanganui; (3) synsedimentary deposits associated with active faults off the northern Manawatu and offshore of Patea; and (4) potentially within buried sand ridges, beach strandlines and paleo-channels on the mid-shelf off Patea and Wanganui.

## 5 Ironsand Distribution

### 5.1 Origin of offshore ironsand deposits

The coastal ironsands of the central North Island west coast are primarily derived from the andesites from the Taranaki volcanics, as strongly suggested by their mineral assemblages (Matthews, 1977, 1979) and by the dispersal trends in ironsand concentration (Hutton 1940; Fleming, 1953; Kear, 1965; Christie, 1975; Carter, 1980). Ironsands on the continental shelf also display a strong Taranaki volcanic provenance, as shown by the concentrations immediately north and south of Cape Egmont. Local fluxes of ironsand, for example off the Mokau River, suggest input from other sources, such as recycling of older, onshore sand deposits (Kear, 1965, 1979).

### 5.2 Surficial distribution

Ironsand concentration maps presented in Carter (1980) show the distribution of ironsand along the North Island west coast (Appendix D). Sediments containing >5% ironsand are spatially restricted to the inner and middle shelves off Auckland, Taranaki and Wanganui. Elsewhere, ironsand contents are low (<2%), with a slight increase in concentration to 2-4% off Kawhia Harbour. A narrow belt extends from the mouth of the Waikato River to just south of Kaipara Harbour, in water depths of 20-40 m. Carter (1980) records the highest ironsand concentration of 39% near the Waikato River mouth and a gradual decrease to the northwest. In contrast, concentration gradients to the southeast and offshore are steep, and the iron-rich belt is strongly delineated.

A second prominent coast-parallel belt exists in the North Taranaki Bight, from Cape Egmont to Tirua Point in depths of 40 m and shallower. Locally, ironsand concentrations reach maximum values off New Plymouth (65%) and the Mokau River (36%), from which concentrations gradually diminish northward (Carter, 1980).

Carter (1980) describes a third southern belt in the South Taranaki Bight, offshore of Patea, reaching a maximum concentration of 22%, but ironsand concentrations >5% persist southeastward along the coast to offshore Wanganui. An offshore belt, with lower ironsand concentrations (1-5%), extends from Cape Egmont to Auckland in depths of 75-100 m.

TTR commissioned XRF analysis of 151 NIWA sediment samples to confirm previous iron oxide concentrations and improve the spatial coverage of data (Appendix D). Both grab and core samples were included. The average  $\text{Fe}_2\text{O}_3$  concentration was 7% and attained a maximum of 35%. These results are broadly consistent with the findings of Carter (1980). Of relevance to the TTR permit areas, the inner shelf off Hawea shows high concentrations of iron oxide, with several surface sediments returning values >10%. This is likely a function of the close proximity of ironsand-rich source rocks, delivered to the coast by the multitude of rivers that drain the Mt Taranaki volcanic complex and ironsand-rich, coastal sedimentary deposits. Bathymetric gradients steepen westward approaching Cape Egmont, which may limit the ability to develop beach-face sand deposits that prograde onto the shelf and will limit the breadth of sediment supply by littoral transport. Furthermore, lahars associated with Mt Taranaki extend out onto the inner-shelf south of the mountain's flanks (Nodder, 1990; Nodder et al., 1992; Nodder, unpublished data).

A comparison of the surficial ironsand concentration (after Carter, 1980) and seismic facies (this study) shows that the highest ironsand concentrations are associated with the Holocene mud/sand wedge. The belt of ironsand enrichment follows a similar coast-parallel geometry as the isopach thickness, whereby the highest concentrations occur where the shore-connected Holocene wedge thickness is generally >3 m.

### 5.3 Sub-surface distribution

As is evident from NIWA core N672 at 93 m water depth from the North Taranaki Bight, a typical core sequence that is ironsand-rich at its base, consists of fine and very fine terrigenous sand, overlying shell-bearing sand (cf. Carter, 1980). Grain size and shell-gravel content broadly increase down-core. Radiocarbon ages on the shell material documented in Norris (1972) and Carter (1980) indicate a range of ages from 8,140 to 19,700 years before present. Carter (1980) interprets these ages to represent deposition of successive transgressive sand sheets across the continental shelf (cf. Norris and Grant-Taylor, 1989). The muddy sands which locally cap the sheet are interpreted as recent sediment, deposited since sea level reached its present level around 6,500 years ago (Gibb, 1979). Gillespie et al. (1998) also show that there is a modern mica-rich sandy mud (or muddy sand) capping the coarser grained deposits especially in the western areas of the Wanganui Bight. Glacio-eustatic sedimentation on the South Taranaki and Wanganui shelves has occurred against a backdrop of regional subsidence, at a rate of around 2.8 m/1,000 years for the last 20,000 years (e.g. Norris and Grant-Taylor, 1989; Nodder et al., 2007).

Carter (1980) suggests that the aerial distribution of ironsand a few metres below the seabed broadly resembles that of the surficial sediments, that is, highest concentrations occur north of Cape Egmont and ironsand concentration diminishes seaward. The suite of shelf cores summarised in Carter (1980) show that measured iron concentrations are variable, but can show increases down-core. This trend appears to be less apparent nearer the shore, with sustained elevated levels (1.1-6.2%) throughout the core, with a relative enrichment in ironsand in the shell/gravel lag at the base.

The selection of XRF analysed samples indicates similar down-core variability in the concentration of magnetic minerals (Appendix D), presumably a reflection of the condensed and mixed lithological lags that make up the coarse-grained deposits on the mid-shelf.

Down-core photographic logs of two giant piston cores (MD06-2993 and MD06-2994, 13 m and 12 m in length, respectively) collected on the northern Manawatu coast (and very close to the southern boundary of permit area 50383 and 54272) during the R/V *Marion-Dufresne* MD152 research voyage (Proust et al., 2006) show that dark, ironsand-rich deposits persist to the base of the cores (locations shown in southern permit area seismic acoustic facies map, Appendix C). This confirms that thick synsedimentary deposits are associated with tectonic deformation in the area, as described in the following section.

Since 2009, TTR have initiated a vigorous drilling programme totalling 777 short core sites (max 16 m core length) and 15 long cores (max 30 m core length) (locations shown on map, Appendix F). Sediment samples taken from specific depth horizons (typically at 1-m interval composites) were assayed for iron content. Collectively, five smaller sub-regions are outlined within the permit areas, with drill statistics and geometric parameters as summarised in Table 5-1 below.

<b>Mining Block</b>	<b>Area (km<sup>2</sup>)</b>	<b>Indicative Fe head grade (%)</b>	<b>Estimated concentrate (megatonnes)</b>	<b>Indicative mine block thickness (m)</b>	<b>Water depth (m)</b>
Xantia	14.98	9.75	10.8	3.3	17 - 32
X2	4.96	12.78	7.7	7.5	25 - 38
Dianne	15.53	10.41	19.9	8.4	21 - 41
D2	3.00	< 9.00	3 - 4	2 - 5m	19 - 25
Christina	15.16	8.75	15	7.8	35 - 42

**Table 5-1: Statistics for each of the five mining areas identified by TTR.**

## 6 Sub-surface geological structure

In the South Taranki Bight, the shallow geological structures are complex (Appendix C). Lamarche et al. (2005) and Nodder et al. (2007) have identified several offshore faults at the seabed associated with the low-strain, compressional Kapiti-Manawatu Fault System, which comprises high-angle (>60°) reactivated reverse and normal faults orientated NE-SW, highly oblique to the northern Manawatu coast. Scarps range from <10–50 km in length, with vertical offsets of 2–30 m. Lamarche et al. (2005) and Nodder et al. (2007) estimate that the Quaternary vertical slip rates are typically <1 mm/y, but may attain 3 mm/y.

In some cases, fault activity has deformed the seafloor, forming scarps that can be imaged in seismic surveys. A shore-normal boomer profile off Himatangi Beach, described by Nodder et al. (2007) from just south of the permit area, shows the development of a thick, shore-attached wedge that tapers seaward onto the emergent trace of the Rangitikei Fault (Figure 6-1). The upper surface of the wedge is locally deformed by the Rangitikei Fault, with thick post-glacial deposits occurring immediately seaward along the footwall of the fault. A deposit at the footwall of the fault attains around 20 m in thickness, but is of limited lateral extent, confined by the local deformation and creation of accommodation space by the recent tectonic deformation.

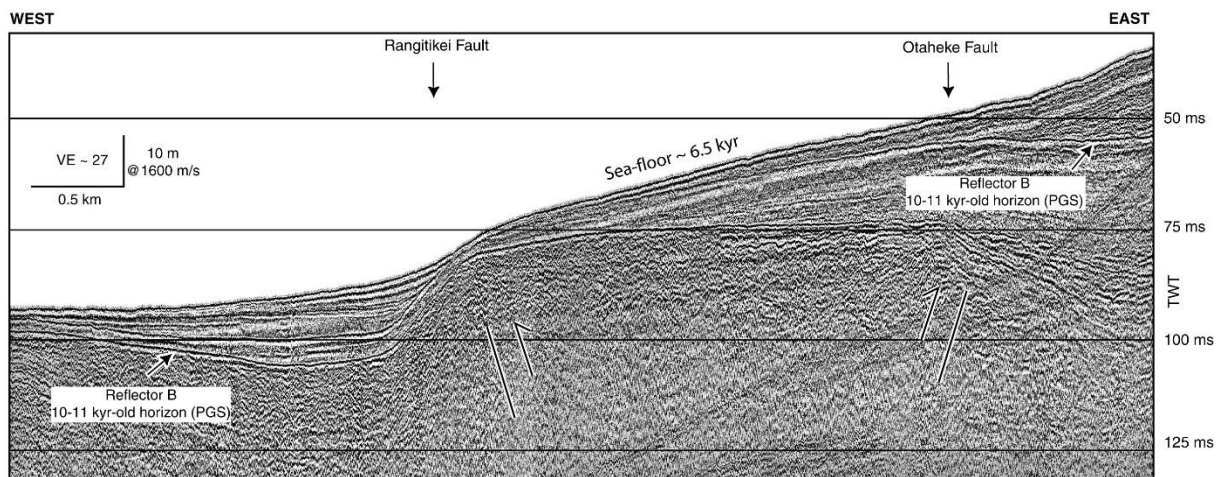


Figure 6

**Figure 6-1: Boomer profile across the shore-attached sediment wedge off the northern Manawatu coast from Nodder et al. (2007).**

On the northern Manawatu coast at the southern limit of the permit area, boomer profiles described by Nodder et al. (2007) suggest synsedimentary thickening of sub-surface reflectors since the last glacial, although the age of the reflectors is inferred and remains problematic (Figure 6-2). Here, the broad seafloor scarp and thick synsedimentary wedge is associated with the Mascarin Fault deformation around 17 km seaward of Tangimoana at 40°16' S. At this location, there is potentially 10+ m of post-glacial sediment. Nodder et al. (2007) infer that paleochannels (white lines on Figure 6-2) that have eroded into gently-dipping sub-bottom reflectors were cut either during the last glacial lowstand (around 18,000 years ago), or during various stillstands during the subsequent sea-level transgression.

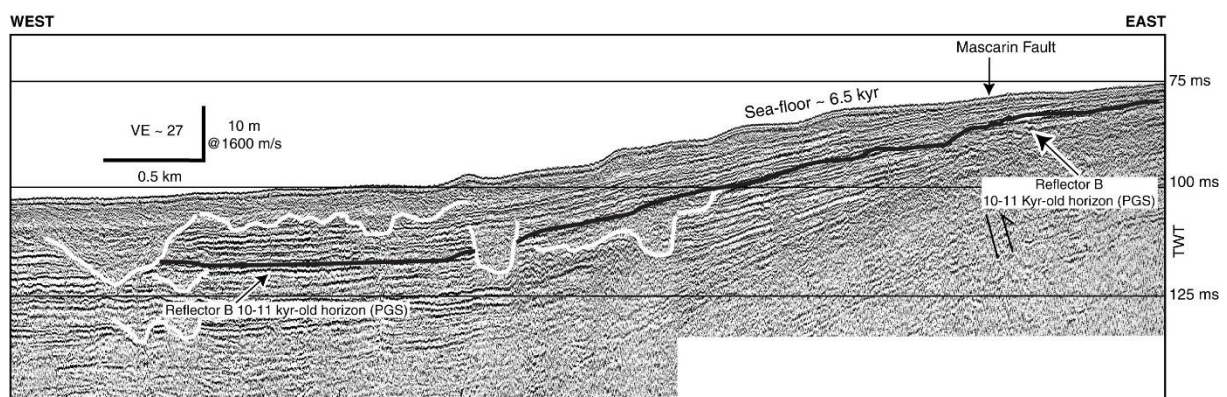


Figure 9

**Figure 6-2: Boomer seismic profile from Nodder et al. (2007) showing a broad seafloor scarp and thick synsedimentary wedge.**

Offshore of Patea and Hawea, there are a number of large faults associated with the structure of Patea-Tongaporutu High (Anderton, 1981; Katz and Leask, 1990, Proust et al., 2005). The northern extension of the Manaia Fault and southern extension of the Taranaki Fault are dominant N-S trending structural lineaments on the western boundary of the Wanganui Basin. However, a significant number of basement structures do not offset overlying late-Quaternary sediments (Proust et al., 2005).

Unpublished surface and near-surface fault data from recent NIWA geophysical voyages are included on the acoustic facies map (Appendix C). Faults were mapped using boomer seismic reflection data. The boomer system is well suited to acoustically penetrate the highly-reflective coarse grained shelf deposits because it has a lower frequency acoustic source than the high-resolution 3.5 kHz system used to identify the near-surface sediment facies described above. Off Patea, these data show N-S trending fault splays, at different stratigraphic levels, in the hanging wall of the large Taranaki Fault (Figure 7-1; Appendix C). Interpreting the full geometry of these smaller structures is problematic, but they could be normal bending moment faults or relaxation structures on top of an uplifted basement high (e.g. Pillans, 1990). Similar to structures observed off the northern Manawatu coast (Figure 6-1 and Figure 6-2), and of relevance to the current study, is the occurrence locally of synsedimentary deposits associated with faults that displace post-glacial sediments. Here, thick deposits occur at the footwall along the more active fault splays and in zones of tectonic deformation.

The N-S strike of the faults along the western boundary of the Wanganui Bight might have cross-cut littoral transport paths, trapping sand in fault-controlled basins. Similarly, along the northern Manawatu coast, fault traces intersect littoral transport paths, but are highly oblique to the modern coastline (e.g. Nodder et al., 2007). Nonetheless, displacement on these faults has created accommodation space that has been infilled by sandy beachface deposits.

The volume of synsedimentary, fault-related deposits are difficult to ascertain for two reasons. Firstly, fault geometry is highly variable along strike of the fault lineament, and secondly post-glacial age control is problematic. Nonetheless, given that most of the other coarse-grained seafloor deposits are generally <3 m in thickness, synsedimentary deposits do represent potentially thick accumulations of ironsand at inner-shelf water depths, as suggested by the two giant piston cores MD06-2993 and MD06-2994.

## 7 Aerial magnetic coverage for the South Taranaki Bight

### 7.1 Background

Aerial magnetic data were integral to the prospecting design and strategy for TTR's assessment of the potential resource. This remote-sensing technique offered many advantages:

- Ability to characterise large areas of the tenements efficiently.
- Could be calibrated and ground-truthed against measured ironsand concentrations.
- Identified 2D and 3D high-magnetic targets for shallow and deep drilling campaigns.
- Provided a baseline dataset that had the potential to readily underpin a broad quantitative assessment of the resource, critical to fulfil The Australasian Code for Reporting of Exploration Results, Mineral Resources and Ore Reserves (Joint Ore Reserves Committee "JORC" Code) requirements.
- Provided insights of depositional models of the resource, and
- Help distinguish modern and ancient depositional environments.

### 7.2 Analysis of archival aerial magnetic coverage and NIWA high-resolution 3.5 kHz seismic reflection profiles offshore of Patea

TTR provided a geo-referenced aerial magnetic image from the Patea region, originally collected by the petroleum industry, and reprocessed at TTR's request by GNS Science in 2009, to enhance near-surface sediment response of filtered aerial magnetic data. Limited background information was provided from TTR about these data, but a discussion with Dr Bryan Davy (GNS Science) – who modified the data for TTR – suggested that: (1) the data presented have been filtered to reflect the magnetic properties of the sediments within the top tens of metres of seafloor sediment; (2) the large processing artefact (dipole) that occurs at the coastline results from topographic effects, i.e. the coastal cliff; and (3) red and blue colours represent positive and negative magnetic anomalies, respectively. The magnetic survey covers ~820 km<sup>2</sup> of the continental shelf (Appendix E). Magnetic anomalies are clearly evident, the most prominent being a sinuous, near-continuous feature, around 200 m in width, which extends southwest across the shelf from the mouth of the modern Patea River. Short, discontinuous segments also occur to the west. A number of anomalies are concentrated in the southwest sector of the coverage, occurring as irregular, broader features, some with north-south lateral extent. In plan form, the sinuous anomalies are geometrically similar to a meandering river channel, whilst linear features have geometries of coarse-grained bars or exposed bedrock ridges.

To investigate these features further, TTR requested an analysis of available seismic reflection data over the magnetic anomalies. The seismic sections available in NIWA's archive are limited to high-resolution 3.5 kHz profiles (analogue only, multiple voyages) and low-frequency single- and multichannel-airgun seismic (primarily NIWA voyage CR3048). The high-resolution 3.5 kHz acoustic system is ideally suited to soft muddy substrates and

can achieve acoustic penetration depths in excess of 50 m in ideal conditions. Owing to the systems high operating frequency, it also can resolve sedimentary units <1 m in vertical thickness. However, coarse gravel and sand substrates are highly reflective and subsurface acoustic penetration is typically masked by prolonged echoes, as is the case for much of the shallow region of the South Taranaki and Wanganui bights (e.g. Table 4-1). The airgun system has been more commonly used for deep seismic surveys (e.g. voyage CR3048; Proust et al., 2005; Lamarche et al., 2007) and has a limiting vertical resolution of 8-10 m. Near-surface sediment geometries can be particularly problematic to resolve in shallow water (<20 m) and as such these data were not analysed in any detail. A “boomer seismic” system is better suited to these substrates, and TTR subsequently contracted NIWA in Aug 2012 and Feb 2013 to collect a selected grid of boomer profiles across magnetic targets (Lamarche et al., 2012; Woelz and Wilcox, 2013).

Within 4 km from the shoreline, 3.5 kHz data show evidence of outcropping Plio-Pleistocene bedrock, a strong seabed reflector, and a rugged seabed with relief up to 10 m (CR3048, Line 15, Appendix E). Here, the wave-abraded mudstone bedrock could be exposed or covered by a very thin veneer of sand, perhaps at most decimetres in thickness in places, and likely occurring as mobile bedforms and ribbons. The red magnetic anomalies coincide with undulating to dipping internal strata and truncated reflectors at the seabed.

Beyond ~7 km of the shore, post-glacial sediment deposits 1-5+ m in thickness overly the sedimentary bedrock (e.g. CR3048, Lines 16, 11, 10, and 7), and in some cases bedforms 1-3 metres in size are interpreted on the seafloor (TAN0105, Line 13, profile C–C'). These sediments are post-glacial marine muds, sands and gravels, and are particularly coarse over the shoals of The Rolling Ground (cf. Appendix B and C). The overall geometry of this sedimentary cover is not well resolved within the existing data.

Subsurface reflectors visible in the profiles in the region of the magnetic anomalies are diffuse and discontinuous, and subsurface geometries are not clearly resolved. In Profile CR3048 Line 16, a weak, undulating and discontinuous reflector at ~3 m depth coincides with the sinuous, strong magnetic anomaly, but no subsurface reflector coincides with smaller anomaly to the east. Similarly, in Profile CR3048 Line 10 (Profile D–D'), a weak, prolonged reflector at ~3 m depth coincides with the western and eastern occurrence of long, sinuous anomalies. The width of strong positive magnetic signature is narrower than the area of sedimentary cover interpreted in the profile. The geometry of these subsurface reflectors is convex-up, with a width of 800 m in the west and 500 m in the east. At the centre of Profile D–D', no subsurface reflector appears to coincide with the small oblate-shaped anomaly. At the seaward extent of the coverage, CR3048 Line 7 traverses a complex array of magnetic anomalies, including long-sinuous features and more irregular shapes. A diffuse subsurface reflector at ~8 m depth coincides with the irregular western anomaly (Profile E–E'). Further east in Profile F–F', a shallow, weak and diffuse reflector dips eastward at the location of a sinuous magnetic anomaly, reaching 11 m depth at the western edge of a second sinuous magnetic anomaly. In Profile G–G', no subsurface reflectors are evident. It is possible that this reflector marks the top of the eroded bedrock sequence beneath a cover of unconsolidated sediment, or it is a reflector within the bedrock sequence itself. No subsurface reflectors are resolved in Profiles C–C' and H–H' in TAN0105 Line 13. However, further west along the survey track in Profile I–I', a sub-horizontal reflector of variable character occurs at around 3 m depth, possibly the post-glacial erosion surface on the

underlying sedimentary bedrock. This surface is also seen in CR3048 Line 11, with variable sediment cover (e.g. Profile K–K'). Here, the magnetic anomalies coincide with areas of the seafloor overlain with a post-glacial deposit up to 3 m in thickness, but also areas with a possible thin veneer of post-glacial sediment, which is too thin to resolve in the seismic profiles.

Post-glacial sediment thicknesses over the wave-abraded erosion surface are variable, consistent with our knowledge of the inner shelf of the Wanganui Bight in general. Magnetic anomalies can coincide with some sub-surface reflectors, but no consistency in sub-surface geometry, or seismic echo character, is evident. As such, these existing 3.5 kHz data alone are not sufficient to confirm or deny the presence of a meandering channel-fill complex.

Orpin et al. (2009) noted that the following geological considerations were potentially relevant to the ongoing interpretation of the magnetic anomalies:

- A lack of appropriate seismic reflection profiles precluded a more conclusive analysis in 2009. [TTR subsequently contracted NIWA in Aug 2012 and Feb 2013 to collect a selected grid of boomer profiles across magnetic targets, including those with channel-like attributes; Lamarche et al., 2012; Woelz and Wilcox, 2013].
- The preservation potential of terrestrial geomorphologic features and deposits on the flooded continental shelf likely requires further verification given the several metres of erosion relief observed in semi-indurated mudstone exposed on the inner shelf.
- The impact of episodic sea-level rise on the formation, position, and preservation of fluvial incisions.
- The consistent geometry and magnitude of the sinuous anomalies, across largely exposed sedimentary bedrock on the innermost shelf and post-glacial marine sediments on the mid-shelf.
- Littoral transport along-shore from west of Patea as the primary source of ironsand versus bedload transport to the shoreline directly from the Patea River.
- Upon sea-level rise, the potential significance of fluvial incisions as a sediment trap for ironsand transported in the littoral zone along-shore.
- The potential significance of out-cropping fault scarps controlling the course of rivers that traverse the shelf during sea-level lowstands.

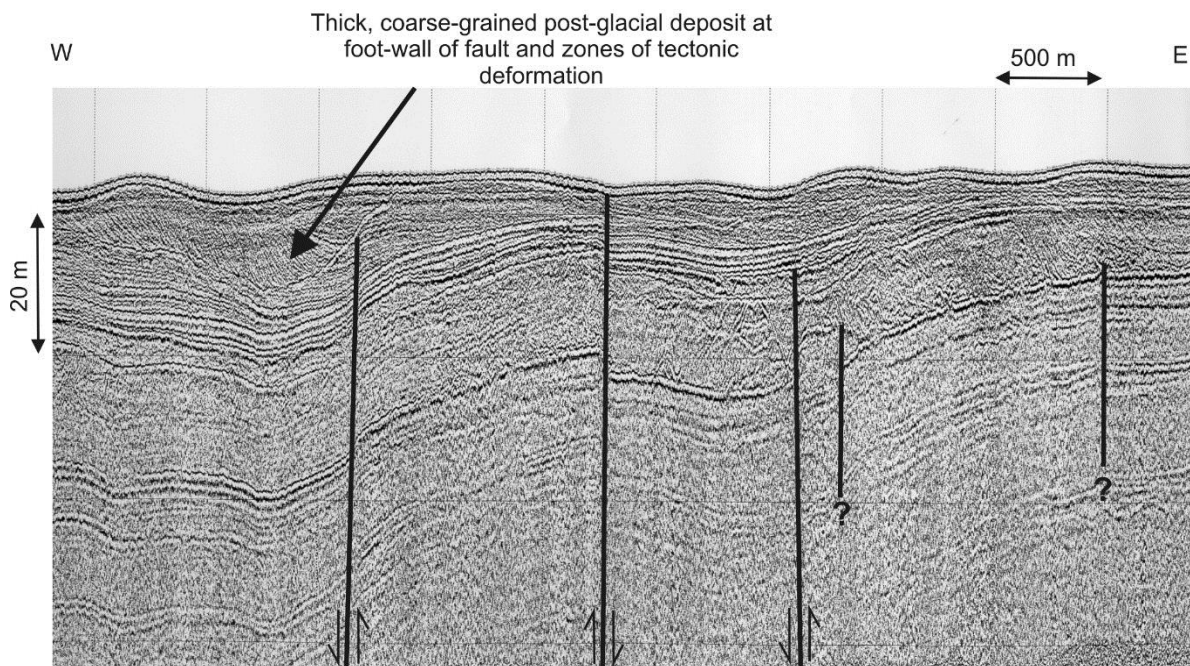


**Figure 7-1: Boomer seismic profile on the mid-shelf off Patea showing small fault splays and active tectonic deformation in the hanging wall of the Taranaki Fault, and thick synsedimentary deposits along the footwalls of the splays.**

## 7.3 Fugro aerial magnetic survey 2010-11

### 7.3.1 Overview

Fugro Airborne Surveys Pty Ltd was commissioned by Trans-Tasman Resources Pty Ltd in 2010–11 to acquire, interpret and model new airborne geophysical data over the prospect permit areas in the northern and southern Taranaki bights (Feijth and Lowe, 2011). Both the 2010 and 2011 inversion were completed with the same resolution (voxel size = 50x50x6m) inversion even though the volume of data more than doubled in 2011. A residual regional grid was produced that represents magnetic sources from the sea floor down to an approximate depth of 600 m, but this deep response was filtered to emphasise the high-frequency magnetic susceptibility to focus on the top 60 m of the sediment pile. The interpretation and inversion modelling was designed to assist target generation for ironsands exploration. This new magnetic surveys was motivated by evidence of discrete zones of enhanced magnetic character over swathes of the prospect areas, and offshore of Patea in particular, as outlined in section 7.2 above.

### 7.3.2 Summary of Fugro's results

There is no definable relationship between magnetic susceptibilities measured on drill samples, using a hand-held magnetic susceptibility meter, and the magnetic susceptibilities generated by the inversion. The mean value of the inversion susceptibilities is 22 times smaller than the mean of the measured susceptibilities. Some scaling of the susceptibilities of the inversion model would be necessary and Feijth and Lowe (2011) indicated that it needs to be investigated when more drill data become available. However, the estimated tonnage of the total iron content calculated from the inversion model is in general agreement with an independent resource model calculated by Golder Associates Pty Ltd over a portion of the Southern permit area for a 5% cut-off grade

Whilst the inversion modelling accurately determines the distribution and position of magnetic sources, including interpreted ironsand deposits, it is not able to resolve the maximum depth extent of these sources. Hence, as noted with the previous magnetic survey data, a composite magnetic character is developed for the upper tens of metres (likely to be <50 m), and is not necessarily restricted to Holocene and late Pleistocene deposits of the last glacio-eustatic sea-level cycle.

Feijth and Lowe (2011) suggested that the newly acquired aerial magnetic data identified similar bedforms and depositional features to those interpreted by Lewis (1979) from shallow-seismic data (Figure 3-1) offshore of Wanganui. The NNW-trending black sand ridges were also remotely sensed as large magnetic bodies, rich in mafic and heavy minerals. These are inferred to be indicators for paleo-shorelines and are characterised by extensive, linear, high frequency, moderate to low amplitude magnetic features, which approximate the present shore line orientation and are sub-parallel to the bathymetry. Ironsand-rich deposits also form as wave-generated strandlines. Prominent E-W trending features were interpreted as paleo-dunes, many of which may only be partially preserved and give rise to more diffuse or discontinuous magnetic patterns.

Feijth and Lowe (2011) suggest that infilled and buried paleo-river channels can be clearly distinguished in the aerial magnetic data, analogous to the older aerial magnetic data discussed in section 7.2 above, and these outline potentially important ironsand-bearing features. Meandering paleo-river channels are characterised by moderate to very high frequency and moderate to high amplitude magnetic responses. Feijth and Lowe (2011) note that although the alluvial appear to be 150 to 200 m wide, according to the inversion model, they may be narrower in reality. Acute features of relative high intensity have been interpreted as the distal parts (edges) of paleo-fan deltas. Sub-linear features of relatively high intensity in this area could either be of alluvial origin or, due to transgression, shallower features of submarine fan deltas.

Feijth and Lowe (2011) also interpreted the location of faults and identified a number of "Tectono-Sedimentary Domains", each with characteristic composite of varying magnetic signatures. Faults, "slump folds", and sub-seafloor structures have been interpreted, along with aeolian dunes, beach ridges and channel systems. Domains with high magnetic signatures helped to establish primary targets for subsequent drilling campaigns by TTR.

With respect to depositional models, Feijth and Lowe (2011) paid particular attention to the potential development of meandering lowstand river channels and contemporaneous ironsand-rich aeolian dunes offshore of Patea. They speculate that the course of the meandering river channel was locally contained within an active graben (interpreted along the margins of the river course from the aerial magnetics by Feijth and Lowe, 2011) prior to transgressive flooding and the present-day highstand (Figure 7-2). Once current highstand conditions were attained ~6,500 years ago, the channel (and presumably the alluvial infill) was buried by a thin cover sequence of sands and gravels, inferred to have been reworked by currents and along-shore drift. In such a scenario, if the lowstand paleo-river channel had incised into the underlying semi-indurated sedimentary bedrock, then this could have improved the chances of preserving the channel base because it would presumably be more resistant to wave-driven erosion than the marginal marine cover sequences. Similarly, if the channel base was lined with fluvial or marginal-marine gravels, bed armouring could have reduced erosion from waves and currents. Coarse-grained deposits do occur at the base of

some cores (e.g. STH0015; Orpin, 2012) but without further verification from a wider suit cores, dates and other sedimentological information, an integrated depositional model remains speculative.

A comparison of the Reduced To Pole 1<sup>st</sup> Vertical Derivative magnetic coverage with unpublished fault data from recent NIWA geophysical voyages (Appendix F) provides an alternative view of near-surface structures. This interpretation suggests that the occurrence and geometry of syntectonic deposits are more complex, possibly of limited lateral extent, and do not necessarily coincide with magnetic anomalies.

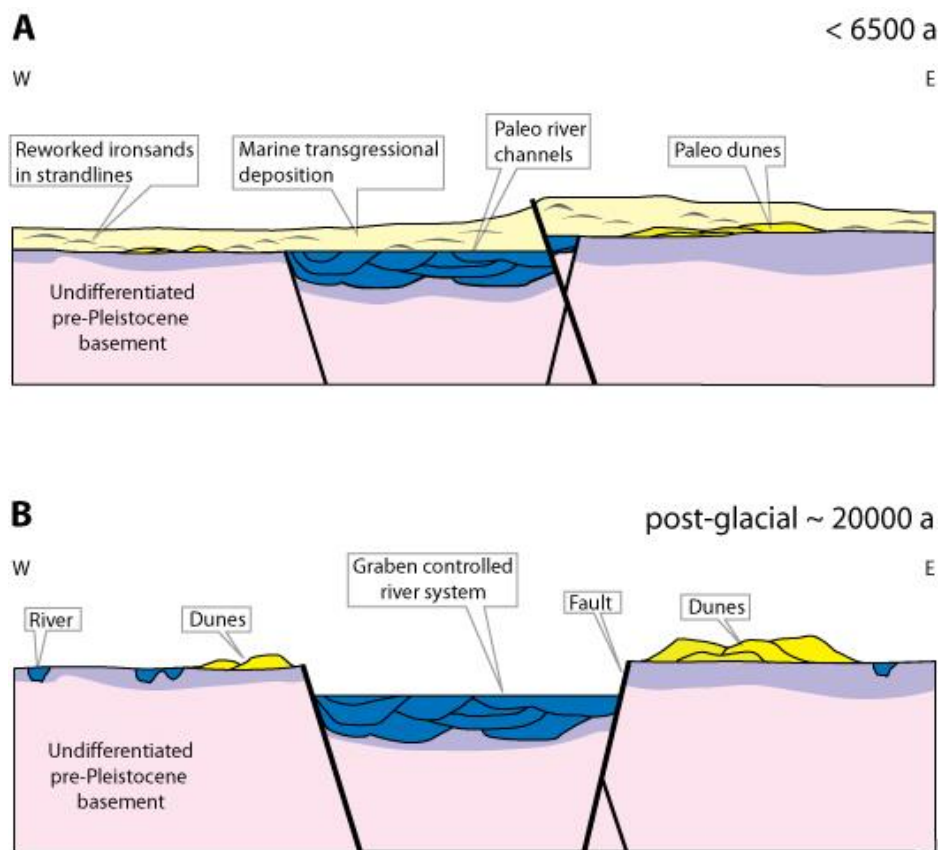


**Figure 7-2: Schematic representation the shelf depositional system on the South Taranaki Bight: (A) <6,500 years ago, and (B) lowstand conditions during the last-glacial maximum ~18,000 years ago. Figure from Feijth and Lowe (2011).**

### 7.3.3 Summary

Sediment supply, lowstand alluvial channel systems and glacio-eustatic sea-level were undoubtedly an important control on the development of the South Taranaki Bight shelf depositional system. Throughout glacio-eustatic cycles, the relative position of the paleo-shoreline would have controlled sediment dispersal and depositional processes, and in turn many of the magnetic anomalies that are inferred to have a geomorphic origin. However, the geomorphic evolution, preservation potential, and sediment sources of some of these deposits, notably the paleo-river channel systems and dunes, remains speculative.

Despite many uncertainties, aerial magnetic anomalies have made a significant contribution to the development of the resource assessment, by enabling TTR to characterise large areas of their tenements and to discriminate areas with potentially high concentrations of ironsand. This underpinning dataset provided targets for coring campaigns that followed, and yielded baseline information that can be readily tested and complimented with other field data and resource models.

## **8 Summary of recommendations arising from 2009 report**

From the overview of the archive information gathered during the initial desktop study, Orpin et al. (2009) recommended that any future survey work in the South Taranaki Bight focus primarily on the following:

- More cores are needed in general to better constrain the three-dimensional variability in ironsand concentration and ground-truth deposits identified in seismic profiles.
- A multibeam bathymetric survey of the ironsand ridges off Wanganui is needed to better constrain their size and extent should seabed mining options be considered preferable to sub-seafloor extraction techniques.
- Synsedimentary deposits associated with active fault deformation could collectively include significant volumes of sand. Their limited lateral extent could offer favourable geotechnical constraints, and as they intersect along-shore littoral transport paths they could be actively replenished. However, estimating their volume would require careful analysis of largely unpublished seismic data to map footwall deposits and along-strike variations in geometry, as well as ground-truthing of the sub-seafloor stratigraphy. This task would represent a new research study.
- A high-resolution seismic survey at the southern permit area is needed to further explore the relationship between river channel-like magnetic anomalies visible in the aerial magnetic data and sub-surface strata. From data collected elsewhere in the Wanganui Bight and northern Manawatu regions, boomer or Chirp seismic reflection is likely the preferred acquisition system to best image coarse-grained substrates in the top 30 m.

Over the intervening four years, TTR have followed a progressive and logical line of enquiry, and have largely actioned these recommendations through their ironsand survey and development programme. NIWA was contracted to provide data in a number of key areas, including:

- Particle size characterisation of sediment samples from cores (e.g. Orpin 2011, 2012, 2013, and laboratory data summaries).
- Sidescan imagery at key exploration sites (Gerring et al., 2012).
- Multibeam bathymetry at key exploration sites (Pallentin et al., 2013).
- Acquisition of high-resolution boomer seismic reflection data at key exploration sites (Lamarche et al., 2012; Woelz and Wilcox, 2013).

Information relating to TTR's additional scientific work undertaken since 2014 has been provided and the conclusions in this report remain valid.

## 9 Bibliography

- Anderton, P.W. 1981. Structure and evolution of the South Wanganui Basin, New Zealand. *New Zealand Journal of Geology and Geophysics* 24, 39–63.
- Arron, E.S., Doyle, A.C. 1982. Raglan Sediments. New Zealand Oceanographic Institute Chart Coastal Series, 1:200,000. DSIR, Wellington.
- Arron, E.S., Doyle, A.C. 1983. Mokau Sediments. New Zealand Oceanographic Institute Chart Coastal Series, 1:200,000. DSIR, Wellington.
- Carter, L, Heath, R.A. 1975. Role of mean circulation, tides, and waves in the transport of bottom sediment on the New Zealand continental shelf. *New Zealand Journal of Marine and Freshwater Research* 9, 423–448.
- Carter, L. (Compiler) 1987. Tasman 2 Cable Route Shallow Water Sector, New Zealand. Pre-Survey Report. A report prepared for Geomex Surveys Pty Ltd. DMFS Contract Report 1987/8, viii + 114 p. + appendices. Lodged at NIWA, Wellington.
- Carter, L. 1980. Ironsand in continental shelf sediments off western New Zealand – a synopsis. *New Zealand Journal of Geology and Geophysics* 23, 455-448.
- Carter, L. 1987. Seafloor sediments and transport. In: Carter, L. (Compiler) 1987. Tasman 2 Cable Route Shallow Water Sector, New Zealand. Pre-Survey Report. A report prepared for Geomex Surveys Pty Ltd. DMFS Contract Report 1987/8, viii + 114 p. + appendices. Lodged at NIWA, Wellington.
- Damuth, J.E., 1980. Use of high frequency 3.5-12 kHz echograms in the study of near bottom sedimentation processes in the deep sea: a review. *Marine Geology* 38, 51–75.
- Doyle, A.C., Arron, E.S. 1982. Raglan Sediments. New Zealand Oceanographic Institute Chart Coastal Series, 1:200,000. DSIR, Wellington.

- Dunbar, G.B., Barrett, P.J. 2005. Estimating palaeobathymetry of wave-graded continental shelves from sediment texture. *Sedimentology* 52, 1–17.
- Ewans, K.C. 1998. Observations of the directional spectrum of fetch-limited waves. *Journal of Physical Oceanography* 28, 495–512.
- Ewans, K.C., Kibblewhite, A.C. 1990. An examination of fetch-limited waves off the West Coast of New Zealand by a comparison with the JONSWAP results. *Journal of Physical Oceanography* 20, 1278–1296.
- Feijth, J., Lowe, S. 2012. Aeromagnetic Interpretation of the Prospecting Permits PP50383 and PP50753, Trans-Tasman Resources Ltd. Fugro PowerPoint presentation of results “2198\_TTR\_2011\_Interpretation\_v3.ppt” supplied to NIWA by TTR, 99pp.
- Fleming, C.A. 1946. Magnetic ironsand-ores west of Wanganui. *New Zealand Journal of Science and Technology, Section B*, vol. 27, 347–365.
- Fleming, C.A., 1953. The geology of the Wanganui subdivision, Waverley and Wanganui sheet districts (N137 and N138). *New Zealand Geological Survey Bulletin* 52, 1–362.
- Gerring, P., MacDiarmid, A., Nodder, S. 2012. Sidescan survey of South Taranaki Sediments. Unpublished NIWA Client Report: WLG2012-17.
- Gibb, J.G. 1978. Rates of coastal erosion and accretion in New Zealand. *New Zealand Journal of Marine and Freshwater Research* 12, 429–456.
- Gibb, J.G. 1979. Late Quaternary shoreline movements in New Zealand. Unpublished Ph.D. thesis, Victoria University of Wellington, New Zealand.
- Gibb, J.G., 1986. A New Zealand regional Holocene sea-level curve and its application to determination of vertical crustal movements. In: Reilly, W.I., Harford, B.E. (Eds.), *Recent Crustal Movements of the Pacific Region*. Royal Society of New Zealand Bulletin 24, 377–395.
- Gillespie, J.L., Campbell, C.S., Nodder, S.D. 1998. Post-glacial sea-level control and sequence stratigraphy of carbonate-terrigenous sediments, Wanganui shelf, New Zealand. *Sedimentary Geology* 122, 245–266.
- Gorman, R.M., Bryan, K.R., Lang, A.K. 2003. Wave hindcast for the New Zealand region: nearshore validation and coastal wave climate. *New Zealand Journal of Marine and Freshwater Research* 37, 567–588.
- Gow, A.J. 1967. Petrographic studies of ironsands and associated sediments near Hawera, South Taranaki. *New Zealand Journal of Geology and Geophysics* 10, 675–695.
- Harris, T.F.W. 1990. Greater Cook Strait – Form and flow. DSIR Marine and Freshwater, Wellington, 212 pp.

- Heath, R.A. 1978. Atmospherically induced water motions off the west coast of New Zealand. *New Zealand Journal of Marine and Freshwater Research* 12, 381–390.
- Heath, R.A. 1982. What drives the mean circulation on the New Zealand west coast continental shelf? *New Zealand Journal of Marine and Freshwater Research* 18, 251–261.
- Heath, R.A., Gilmour, A.E. 1987a. Currents. In: Carter, L. (Compiler) 1987. *Tasman 2 Cable Route Shallow Water Sector, New Zealand. Pre-Survey Report. A report prepared for Geomex Surveys Pty Ltd. DMFS Contract Report 1987/8, viii + 114 p. + appendices. Lodged at NIWA, Wellington.*
- Heath, R.A., Gilmour, A.E. 1987b. Flow and hydrological variability in the Kahurangi Plume off north-west South Island, New Zealand. *New Zealand Journal of Marine and Freshwater Research* 21, 125-140.
- Kear, D. 1965. Geology of New Zealand's ironsand resources. Publications of the 8th Commonwealth Mining and Metallurgical Congress, Australia and New Zealand paper 219, 1-10.
- Kear, D. 1979 (reprinted). Geology of ironsand resources of New Zealand (with notes on limestone, silica and bentonite). A report prepared for NZ Steel Investigating Co. Ltd. Department of Scientific and Industrial Research, vi + 164 pp.
- Kibblewhite, A.C., Bergquist, P.R., Foster, B.A., Gregory, M.R., Miller, M.C. 1982. Maui Development Environmental Study. Report on Phase Two 1977-1981. Prepared by the University of Auckland for Shell BP and Todd Services Ltd. Auckland, October 1982.
- King, P.R., Scott, G.H., Robinson, P.H. 1993. Description, correlation and depositional history of Miocene Sediments outcropping along the North Taranaki coast. Institute of Geological and Nuclear Sciences Monograph 5, GNS Science, New Zealand.
- King, P.R., Thrasher, G.P. 1996. Cretaceous-Cenozoic geology and petroleum systems of the Taranaki Basin, New Zealand. Institute of Geological and Nuclear Sciences monograph 13.
- Lamarche, G., Proust, J.-N., Nodder, S.D. 2005. Long-term slip rates and fault interactions under low contractional strain, Wanganui Basins, New Zealand. *Tectonics* 24, TC4004, doi:10.1029/2004TC001699.
- Lamarche, G., Wilcox, S., Woelz, S. 2012. High-resolution boomer survey in South Taranaki Bight. Unpublished NIWA Client Report WLG2012-46, 38pp.
- Lewis, K.B. 1979. A storm-dominated inner shelf, western Cook Strait, New Zealand. *Marine Geology* 31, 31–43.
- Lewis, K.B. 1994. The opening of Cook Strait: Interglacial tidal scour and aligning basins at a subduction to transform plate edge. *Marine Geology* 116, 293–312.

- Lewis, K.B., Mitchell, J.S. 1980. Cook Strait Sediments. New Zealand Oceanographic Institute Chart Coastal Series, 1:200,000. DSIR, Wellington.
- Matthews, E.R. 1977. The movement of sand on some western Taranaki beaches. Unpublished MSc thesis, University of Auckland, New Zealand.
- Matthews, E.R. 1979. Seasonal variation in volume and morphology of some western Taranaki Beaches. *New Zealand Journal of Geology and Geophysics* 22, 465-472.
- Mauk, J.L., Macorison, K., Dingley, J. 2006. Geology of Waikato Head and Taharoa Ironsand deposits. In: A.B. Christie and R.L. Brathwaite (editors), *Geology and Exploration of New Zealand Mineral Deposits*. AusIMM Monograph 25, p.231–234.
- McDougall, J.C. 1961. Ironsand deposits offshore from the west coast, North Island, New Zealand. *New Zealand Journal of Geology and Geophysics* 4, 283–300.
- McDougall, J.C., Brodie, J.W. 1967. Sediments of the western shelf, North Island, New Zealand. *New Zealand Oceanographic Institute Memoir* 40, 56 pp.
- Nodder, S.D. 1990. Report for NZOI Oceanographic Research Voyage CR2033. Unpublished data, NIWA, Wellington.
- Nodder, S.D. 1993. Neotectonics of the offshore Cape Egmont Fault Zone, Taranaki Basin, New Zealand, *New Zealand Journal of Geology and Geophysics*, 36:2, 167–184.
- Nodder, S.D. 1995. Late Quaternary transgressive/regressive sequences from Taranaki continental shelf, western New Zealand. *Marine Geology* 123, 187–214.
- Nodder, S.D., Edwards, N.A., Burrows, M.W. 1992. Patea Sediments, 2nd Edition. *New Zealand Oceanographic Institute Chart Coastal Series*, 1:200,000. DSIR, Wellington.
- Nodder, S.D., Lamarche, G., Proust, J.-N., Stirling, M. 2007. Characterizing earthquake reoccurrence parameters for offshore faults in the low-strain, compressional Kapiti-Manawatu Fault System, New Zealand. *Journal of Geophysical Research* 112, B12102, doi:10.1029/2007JB005019.
- Norris, R.M. 1972. Shell and gravel layers, western continental shelf, New Zealand. *New Zealand Journal of Geology and Geophysics* 15, 572-589.
- Norris, R.M., Grant-Taylor, T.L. 1989. Late Quaternary shellbeds, western shelf, New Zealand. *New Zealand Journal of Geology and Geophysics* 32, 343–356.
- Orpin, A. 2011. Schedule N: Sediment characterization analysis: particle size of samples from RC core STH004. Unpublished NIWA Client Report: WLG2011-44.
- Orpin, A. 2012. Schedule N, Part 2: Sediment characterisation analysis: particle size of samples from cores STH010RC and STH012RC. Unpublished NIWA Client Report: WLG2012-23.

- Orpin, A. 2013. Schedule AG. Sediment characterization: Textural comparison of grab and spear samples from RC cores. Unpublished NIWA Client Report: WLG2013-28.
- Orpin, A., Bostock, H., Bardsley, S., MacKay, K. 2009. Offshore Desktop Study of Prospecting Permits PP 50383 and PP 50753, North Island West Coast. Unpublished NIWA Client Report WLG2009-21, 45pp + 5 appendixes.
- Pallentin, A., Gerring, P., Woelz, S., Fenwick, M. 2013. Multibeam survey in South Taranaki Bight. Unpublished NIWA Client Report: WLG2013-8.
- Perrett, T.L. 1990. Variations in sediment texture and biota off a wave-dominated coast, Peka Peka, New Zealand. Unpublished MSc thesis, Victoria University of Wellington, 135 pp.
- Pickrill, R.A., Mitchell, J.S. 1979. Ocean wave characteristics around New Zealand. *New Zealand Journal of Marine and Freshwater Research* 13, 501–520.
- Pillans, B. 1990. Vertical displacement rates on Quaternary faults, Wanganui Basin, *New Zealand Journal of Geology and Geophysics* 33, 271–275.
- Proctor, R, Carter, L. 1989. Tidal and sedimentary response to the late Quaternary closure and opening of Cook Strait, New Zealand: results from numerical modelling. *Paleoceanography* 4, 167-180.
- Proust, J.-N., Lamarche, G., Migeon, S., Neil, H. 2006. Campagne GEOSCIENCES; MD 152 (24 January- 7 February 2006) on R/V Marion-Dufresne. "Tectonic and climatic controls on sediment budget". Institut Paul Emile Victor (IPEV) voyage report, No. 108 p. IPEV, Brest, France.
- Proust, J.-N., Lamarche, G., Nodder, S.D., Kamp, P.J.J. 2005. Sedimentary architecture of a Plio-Pleistocene proto-back-arc basin: Wanganui Basin, New Zealand. *Sedimentary Geology* 181, 107–145.
- Stokes, S., Nelson, C.S., Healy, T.R., MacArthur, N.A. 2006. The Taharoa ironsand deposit. In: A.B. Christie and R.L. Brathwaite (editors), *Geology and Exploration of New Zealand Mineral Deposits*. AusIMM Monograph 25, p.105–109.
- Sutton, P.J.H., Bowen, M.M. 2011. Currents off the west coast of Northland, New Zealand, *New Zealand Journal of Marine and Freshwater Research* 45, 609–624, DOI: 10.1080/00288330.2011.569729.
- Woelz, S., Wilcox, S. 2013. High-resolution boomer survey in South Taranaki Bight, 2<sup>nd</sup> survey. Unpublished NIWA Client Report WLG2013-13, 35pp.

## **Appendix A NIWA archive sediment samples**

NIWA archive sediment samples from the North and South Taranaki bights.

## **Appendix B NZOI 1:200,000 Coastal Sediment Chart Series**

Patea Sediments (Nodder et al., 1992)

## **Appendix C 3.5 kHz seismic acoustic facies maps with sediment sample locations**

## **Appendix D Ironsand concentrations and distribution**

## **Appendix E Compilation of archival aerial magnetic coverage and high-resolution 3.5 kHz seismic reflection profiles, Patea**

## **Appendix F Reduced-To-Pole 1<sup>st</sup>-Vertical Derivative magnetic coverage from Fugro aerial magnetic survey with unpublished NIWA fault data**